DESIGN AND OPTIMIZATION OF HYBRID ENERGY STORAGE FOR PHOTOVOLTAIC POWER FLUCTUATION SMOOTHING BASED ON FREQUENCY ANALYSIS

by

Ruirui Yang

A Thesis Submitted in

Partial Fulfillment of the

Requirements for the Degree of

Master of Science

in Engineering

at

The University of Wisconsin-Milwaukee

May 2016

ABSTRACT

DESIGN AND OPTIMIZATION OF HYBRID ENERGY STORAGE FOR PHOTOVOLTAIC POWER FLUCTUATION SMOOTHING BASED ON FREQUENCY ANALYSIS

by

Ruirui Yang

The University of Wisconsin-Milwaukee, 2016
Under the Supervision of Professor David Yu

A proper design of energy storage system (ESS) can effectively smooth the photovoltaic (PV) output power fluctuation, lower the cost, and improve the power quality and stability.

According to the response characteristics of different energy storage equipment, an optimal hybrid EES sizing method is proposed based on frequency analysis. A hybrid ESS including lead-acid battery, lithium battery and electric double-layer capacitor (EDLC) is selected to smooth out PV power fluctuation and meet both power and energy requirement of the power grid. Fast Fourier Transform (FFT) method is applied for analyzing the spectrum of unwanted PV fluctuation. From the FFT analysis, different frequencies combinations can be determined to meet both the power and energy requirements of the potential hybrid ESS solution.

An optimization technique is conducted to find the best frequency combination, hence the best hybrid ESS solution. The goal of the optimization is to minimum total hybrid ESS cost by taking selected ESS cycle life and charge/discharge loss into consideration. The proposed method is based on the worst case scenario of PV fluctuation. Through the proposed method, the least cost

ESS solution will be determined to meet both the power and energy requirements as well as smooth out the PV output fluctuation under the worst case scenario.

TABLE OF CONTENTS

LIST OF FIGURES

LIST OF TABLES

ACKNOWLEDGEMENTS

First of all, I would like to express my heartfelt gratitude to my advisor Professor David Yu for his patient guidance. I sincerely appreciate for all those discussions and meetings in which Professor Yu shared his invaluable knowledge and experience, and helped me to work out difficulties. I feel so lucky and blessed to have such a great advisor who spares no effort to help students. Then I would like to specifically thank Dr. Qiang Fu for his careful guidance, support and encouragement to me, and for his effort to provide useful data and information in this project. I would also like to thank Professor Deyang Qu and Professor Jun Zhang for their insightful ideas and helpful advices in my work.

Additionally, I want to thank my friends for their advice in my work and help in my life, especially thank Bin Chen and Ruijing Yang for their help both in my study and personal life.

Finally, I would like to express my deepest appreciation to my family, for their unconditional love and support, only with their love can I go so far to know more about the wonderful world.

Chapter 1 Introduction

In this chapter, the background, research status, and general approach are presented.

1.1 Background

With the decreasing of fossil fuel, the development of renewable energy has become a tendency nowadays. Among all kinds of renewable energy, solar energy is of the most widely used one. Solar photovoltaic (PV) energy installed capacity over the past decade has risen rapidly. In 2006, the global solar PV energy installed capacity was only 5 gigawatts (GW), while by the end of 2014, the stabilization of solar power over the world was 177 GW according to literature [1].

However, since the PV system output power is easily affected by factors as temperature and illumination intensity, its power fluctuation may probably be harmful to the power grid [2]. New technologies, such as new wind and solar forecasting tools, demand-side control, fast startup units, and many others, have been proposed to address this balancing issue [3]. Among those options, energy storage (ES) is a viable solution because of its fast response and control flexibility [4], [5].

Currently, the industry typically applies a single energy storage (ES) device at the PV location in order to smooth out PV power fluctuation under the worst case scenario. However, this approach

tends to oversize the energy storage system (ESS) and increase its cost.

A hybrid ESS is an effective solution to minimize the power fluctuation caused by the intermittent nature of wind and solar power. For short to mid-term (seconds to minutes) power management, the most commonly seen storage techniques in a PV system are EDLCs. For mid-term to long term (minutes to hours) power management, lead-acid batteries and lithium batteries are most widely used. [2]

By properly integrating different types and capacities of ESS, such as lithium battery and EDLC, the fluctuation of PV output power can be effectively smoothed. Since each energy storage device is of different charging and discharging speed and characteristics, the performance can be enhanced with less cost when operating together.

1.2 Research Status

In this section, PV system will be briefly described, research status of ESS will be presented.

1.2.1 PV System

As shown in Figure 1-1, a PV power generation system consists of PV arrays, ESS, converters, and inverters. PV arrays convert solar energy into electrical energy based on photovoltaic effect.

ESS, which contains hybrid batteries and controlled by certain control method, smooth the grid input power by absorbing excessive power and supply insufficient power of PV output. PV inverters and converters are the applications of power electronic technology. PV inverters adjust the value of direct current (DC) power from PV arrays or ESS to match the voltage of DC bus. PV converters convert DC power generated by PV arrays and ESS into alternating current (AC) power, so that the power can be supplied to the load or incorporated into the power grid.

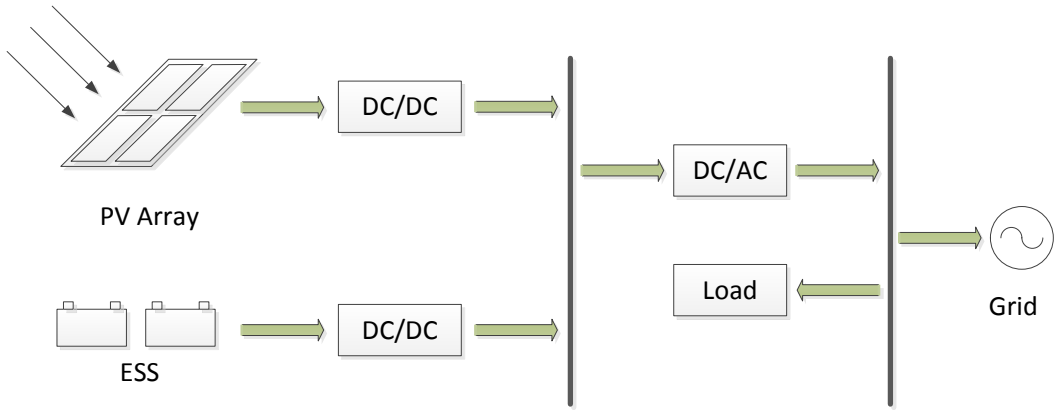

Figure 1-1 PV power generation system structure

PV system can be operated in two modes: grid-tied mode and grid-forming mode. In this paper the research is analyzed based on the assumption that this PV system always operates in grid-tied mode.

The grid input power quality is mainly affected by both capacity design and control method of the ESS. Sizing ESS to accommodate high penetration of variable energy resources based on frequency domain has been conducted in literature [6]. Research on the control method of MPPT

with hybrid energy storage system to smooth the output power fluctuation has been conducted in literature [7]. Also the wavelet packet-fuzzy control of hybrid energy storage systems for PV power smoothing which is conducted in the frequency domain has been proposed in literature [8].

1.2.2 Energy Storage System

There are several suggested methods for categorization of various ESS in terms of their functions, response times, and suitable storage durations [9], [10], [11]. In this paper, ESS is divided into two categories of long-term ES and short-term ES.

(1) Long-term Energy Storage

Long-term ES represent those ES with long response time. The long-term response energy storage devices have the capability to supply or absorb electrical energy during hours. Their power systems application is usually related with energy management, frequency regulation or grid congestion management [12], [13]. The use of long-term energy storage devices is expected to rise in the next years because the generation availability fluctuations associated to the increasing integration of renewable sources in power systems [14].

Electrochemical batteries are one of the most widely used long-term ES. They use electrodes both as part of the electron transfer process and store the products or reactants via electrode solid-state reactions [12]. There are a number of battery technologies under consideration for energy storage, where the main are:

- lead acid
- Nickel cadmium
- Sodium sulphur
- Lithium ion
- Sodium nickel chloride

(2) Short-term Energy Storage

Short-term response energy storage devices should be used to aid power systems during the transient period after a system disturbance, such as line switching, load changes and fault clearance. Their application prevents collapse of power systems due to loss of synchronism or voltage instability, improving its reliability and quality.

Short-term response energy storage devices use is getting common in power systems with important renewable energy penetration like wind and weak interconnections or in islands, avoiding temporary faults and contributing to the provision of important system services such as

momentary reserves and short-circuit capacity [15], [16]. The main short-term energy storage devices and their operation are:

- Flywheels
- Supercapacitors
- Magnetic Superconducting

Supercapacitors are the latest innovational devices in the field of electrical energy storage. In comparison with a battery or a traditional capacitor, the supercapacitor allows a much powerful power and energy density [17].

Supercapacitors are electrochemical double layer capacitors (EDLC) that store energy as electric charge between two plates, metal or conductive, separated by a dielectric, when a voltage differential is applied across the plates. Similar to battery systems, capacitors work in direct current. This fact imposes the use of electronic power systems, as presented in Fig.1-2. [18]

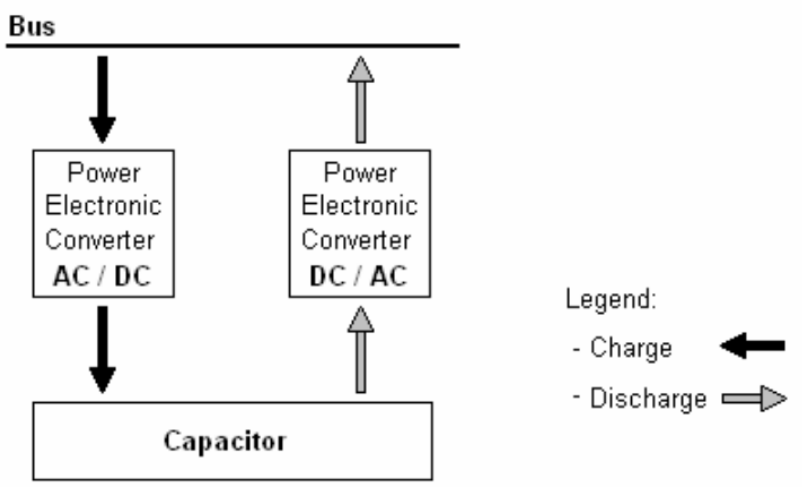

Figure 1-2 Working scheme of capacitor

Supercapacitors find their place in many applications where energy storage is needed, such as uninterruptible power supplies, or smoothing strong and short-time power solicitations of weak power networks. Their main advantages are the long cycle life and the short charge/discharge time. [19]

1.3 Research Objective and Article Layout

Because of its easier integration with existing infrastructure, PV is projected to overtake wind becoming the dominant green energy in the next ten years. In order to achieve this goal, two main technical challenges need to be solved:

- Increase the efficiency of PV output
- Determine a cost effective energy storage (ESS) methodology to handle the intermittency in PV output

The objective of this proposal is to design a right mix of hybrid energy storage devices based on Fast Fourier Transform (FFT) method to effectively smooth the photovoltaic (PV) output power fluctuation as well as to minimize the cost.

This research considers the wide variation in PV intermittency and cost differences among different types of ESS and proposes a systematic strategy to design a cost effective ESS solution to smooth the fluctuation in PV output.

In this paper, the proposed FFT based approach can effectively calculate the complete spectrum of individual components with different frequency which causes the variation in the PV power output. The PV output variation is calculated using year-long PV data measured at an experimental station in Milwaukee in a 24-hour interval. The data has also gone through a statistical analysis in order to select a worst case by taking seasonal and local weather patterns into consideration. A systematic approach is designed using FFT results and matching with available storage devices with different charging and discharging rates in order to determine the most effective ESS solution with lowest cost.

The key idea in the proposal is to divide the complete frequency spectrum of the unwanted PV output variation into several sections. The individual frequency components in each section are accumulated together by a single frequency component with its frequency being equal to or

greater than the highest frequency in the section. Each determined single frequency component represents a required ESS. An optimization technique is applied to determine the most effective ways with minimum cost to divide the entire frequency spectrum and match with the optimal ESS combination with the least cost. Figure 1-3 shows the flowchart and required tasks of the proposed research.

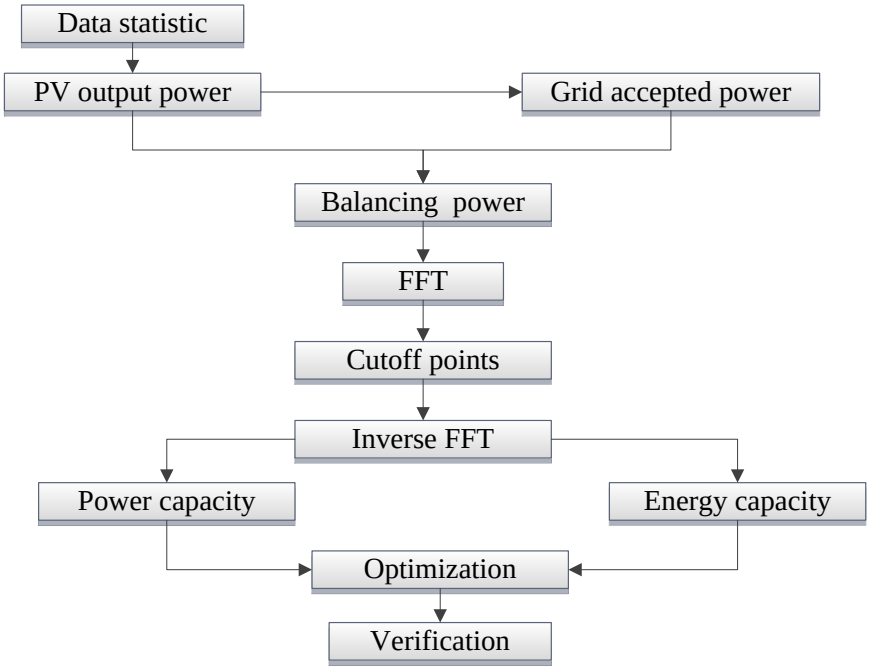

Figure 1-3 Flow chart of proposed research

- Data statistics: Collecting everyday light illumination data in the Milwaukee area. Using the appropriate statistical method to select worst case of PV output power data in all year (5:00 a.m.-8:00 p.m.).
- Calculation of balance power: Calculating the accepted power in the grid based on existing grid input power fluctuation standards. Then balance power can be obtained by using average power minus accepted power.

- FFT method: Conducting FFT algorithm on the calculated balance power to determine the completed frequency spectrum.
- Determination of cutoff points: Based on energy storage devices' characteristics (the rate of charging and discharging) that are already on the market. The cutoff points determine the range of each section.
- Determination of the ESS's capacity: Conducting inverse FFT algorithm in each individual frequency band and the capacity of power and energy can be determined back in the time domain.
- Optimization based on cost: The goal is to make sure that the total cost of total energy storage devices is the lowest. Also make sure that when adding all selected ESSs together, it can cover the entire frequency spectrum.
- Verification: Using practical data to verify the effectiveness of the resulting mix energy storage system.

There are six chapters in this thesis. Chapter 1 introduces the background of both PV system and ESS, and the new progress in the area. Research objectives and article layout are also included in this chapter. Chapter 2 explains the worst case selecting standard, grid acceptable power calculating algorithm, the concept and calculation of balance power, and FFT method. It is the crucial basis for the latter part of the thesis.

Chapter 3 consists both the energy capacity and power capacity design of ESS. And then use the calculated total power and energy capacity to verify the results. Finally, total cost under this design is calculated in this chapter. Chapter 4 illustrates the optimization of total cost by changing cutoff points locations. Cycle life and loss are concluded in the optimization part. Also ESS with three energy storage devices are researched and its total cost is compared with only two ESs. Chapter 5 is composed of the verification of this design. Chapter 6 presents the conclusion and prospects the future work.

Chapter 2 Data processing

2.1 PV Output Power

Using Simulink sample *A 100kW array connected to a 25kW grid via a DC-DC boost converter and a three phase three level VSC* shown in Figure 2-1 as the basic model.

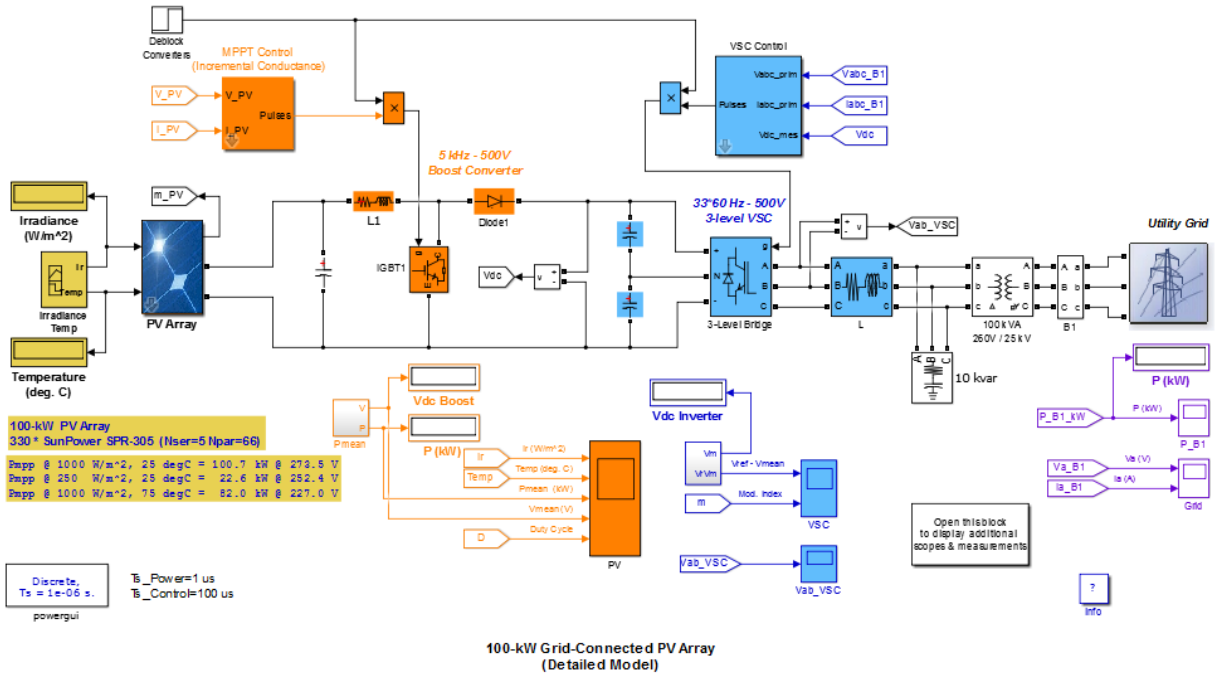

Figure 2-1 100kW Grid connected PV array Simulink model

Several modifications are made for this research. Disconnected PV array and maximum power point tracking (MPPT) control model with transmission lines and power grid by applying several electronics to obtain PV output power directly as shown in Figure 2-2. Since PV output power is mostly affected by light illumination and temperature, to simplified simulation, temperature is set to a constant 25 centigrade, which is the standard temperature.

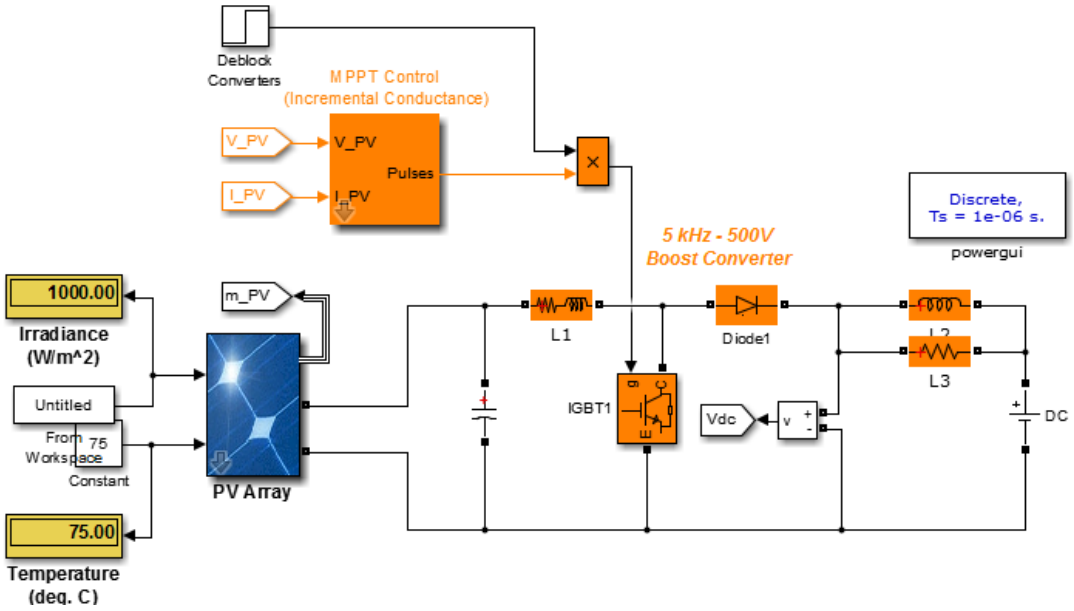

Figure 2-2 PV array Simulink model

Due to the fact that light illumination and the output power is close to linear correlation, and simulation for one-day input data is relatively time consuming using this model, in this paper, one-minute data are used to calculate a proportional coefficient as shown in Figure 2-3.

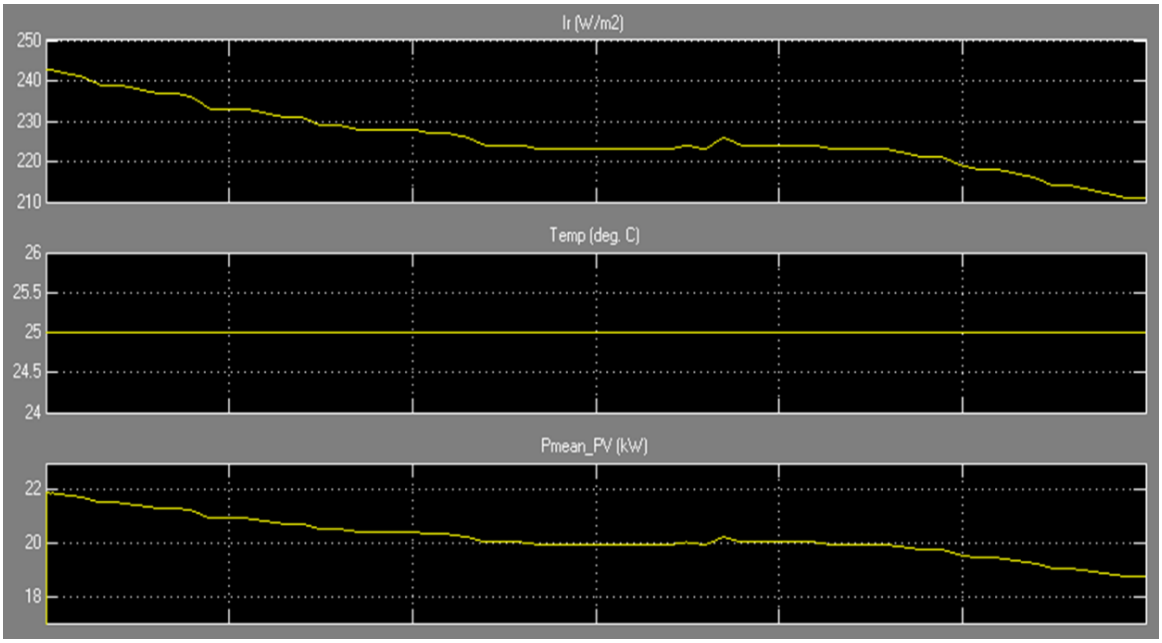

Figure 2-3 PV array simulation result in 1 minute

It can be seen that the result has a high linearity. In Table 2-1 several data are collected to calculate the proportional coefficient *k* of light illumination value and PV output power value.

Table 2-1 Simulation result data

Light illumination	**PV output power**
250 W/m^2	22.6 kW
1000 W/m^2	100.7 kW

$$k = \frac{100.7-22.6}{1000-250} \approx 0.1 \ \ kW/(\frac{W}{m^2}) \quad (2\text{-}1)$$

Based on calculated result, PV output power can be approximately considered as light illumination value multiplied by 0.1.

2.2 Grid Acceptable Power

High penetrations of variable energy resources create significant uncertainty regarding the power generation required to balancing energy production with consumption [20]. Solar power variations are hard to predict and cause multiple impacts including the effect on system reliability[6].

Acceptable refers to the requirement that the system be able to sustain any credible contingency or event without involuntary loss of load. Capacities of ESS are determined based on the grid acceptable power flutuations.

In this research, all data are collected from a small PV station. According to the limit value of power fluctuation as shown in Table 2-2 below, the maximum change of output power, which is the grid input power, is 0.2MW per minute. [21]

Table 2-2 Maximum power variation limit in PV station

PV station type	Maximum power variation in 10min/MW	Maximum power variation in 1min/MW
Small	Installed capacity	0.2
Medium	Installed capacity	Installed capacity/5
Large	Installed capacity/3	Installed capacity/10

Since 200kW is the maximum fluctuation value for 1 minute, and in this research, sample time is 1 second. To simplify the standard, here we assume the maximum fluctuation value for 1 second is 1/60 of the value for 1 minute, which is about 3kW.

The grid acceptable power can be calculated with a certain algorithm using PV output data. As shown in Figure 2-4, the algorithm will calculate the maximum range (as shown in blue box) of power fluctuation that can be accepted by power grid in the next second, which is $\pm$3kW in this case. The original PV output power fluctuation is shown in green line, and red line represent the acceptable power calculated by algorithm.

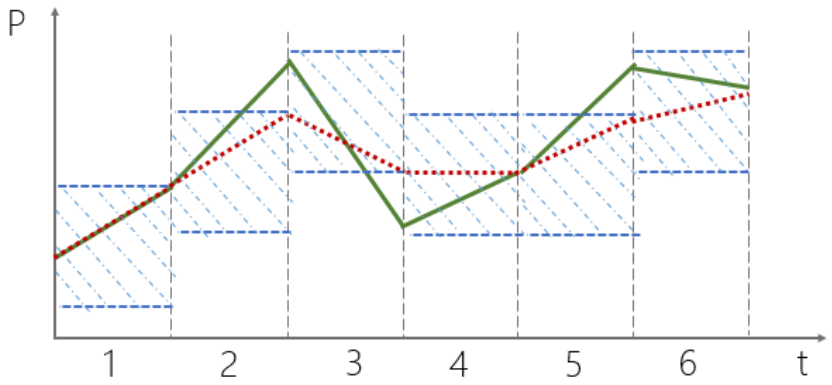

Figure 2-4 Outline of an inductor with core

The algorithm procedures are shown in Figure 2-5. By inputting PV output power data, the grid acceptable power can be obtained as Figure 2-6. According to this algorithm, the next second will be automatically corrected as the maximum or minimum fluctuation value if it is beyond that range (as shown in time interval 2, 3, and 5). Otherwise it will stay the same value as it is (as shown in time interval 1, 4, and 6).

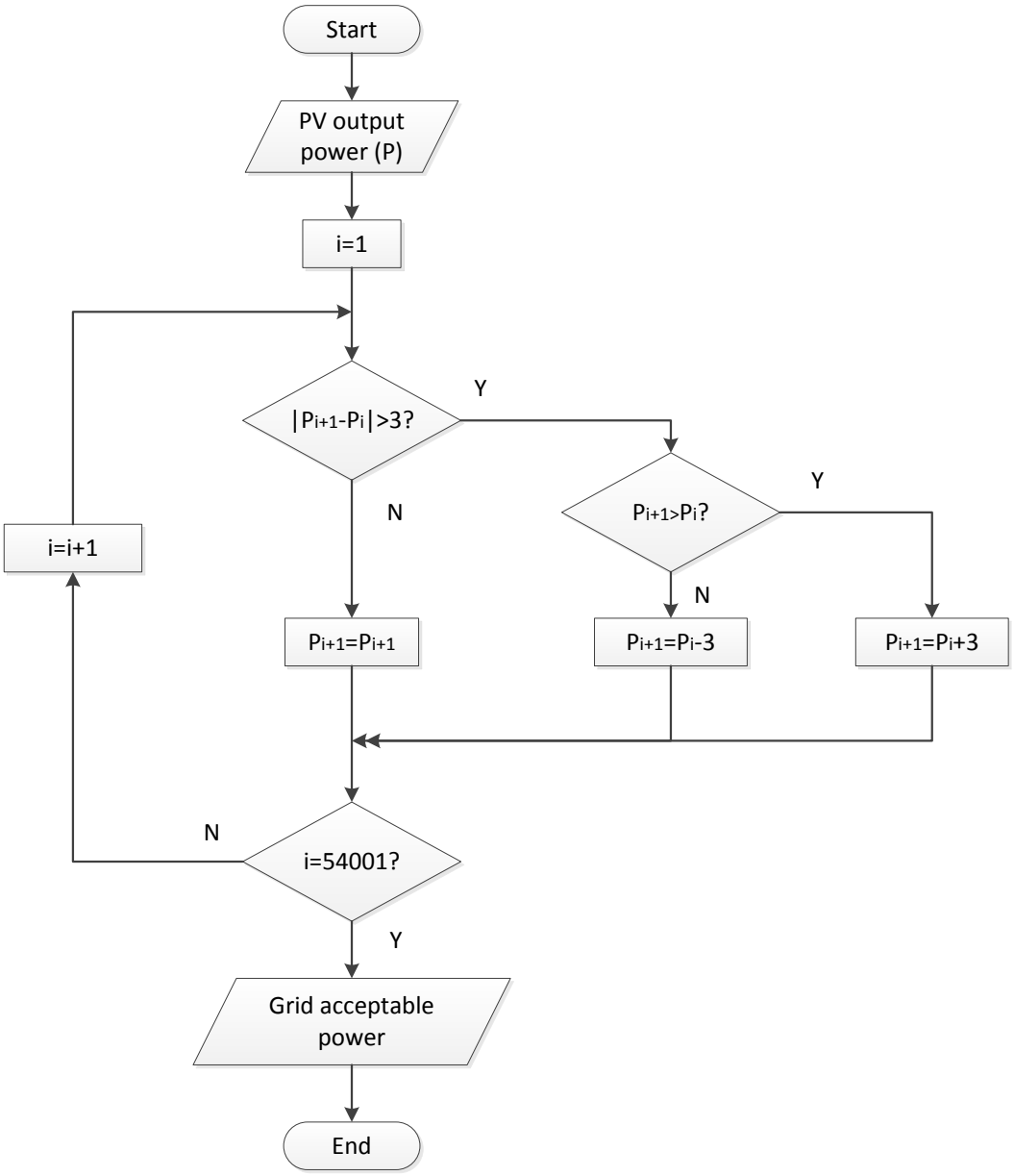

Figure 2-5 Flow chart to obtain grid acceptable power

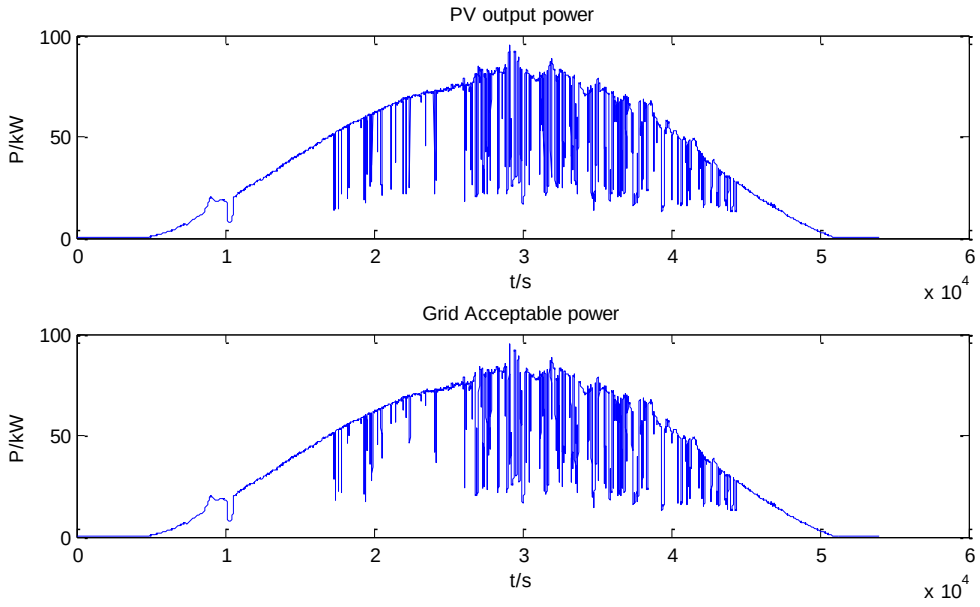

Figure 2-6 Grid acceptable power

2.3 Balancing Power

To meet the requirement of grid acceptable power standard, ESS is applied to maintain the balance between PV output power and grid input power. Toward this end, the notion of system balancing was developed and is used universally in all systems. According to reference [22], balancing represents excess or shortage capacity in the system, either in the form of excess available generation or shortage demand in PV. Balancing power is the key factor of sizing ES capacities.

Based on PV output power P_o, grid acceptable power P_a, the balancing power P_b can be expressed as follows:

$$P_b = P_o - P_a \tag{2-2}$$

Where:

$P_b > 0$: PV generates excess available power which need to be absorbed by ESS.

ES is being charged when $P_b > 0$.

$P_b < 0$: PV generates insufficient available power which need to be supplied by

ESS. ES is being discharged $P_b < 0$.

Balancing power as shown in Figure 2-7 is the selected worst case power required to be smoothed by ESS when PV system is operating.

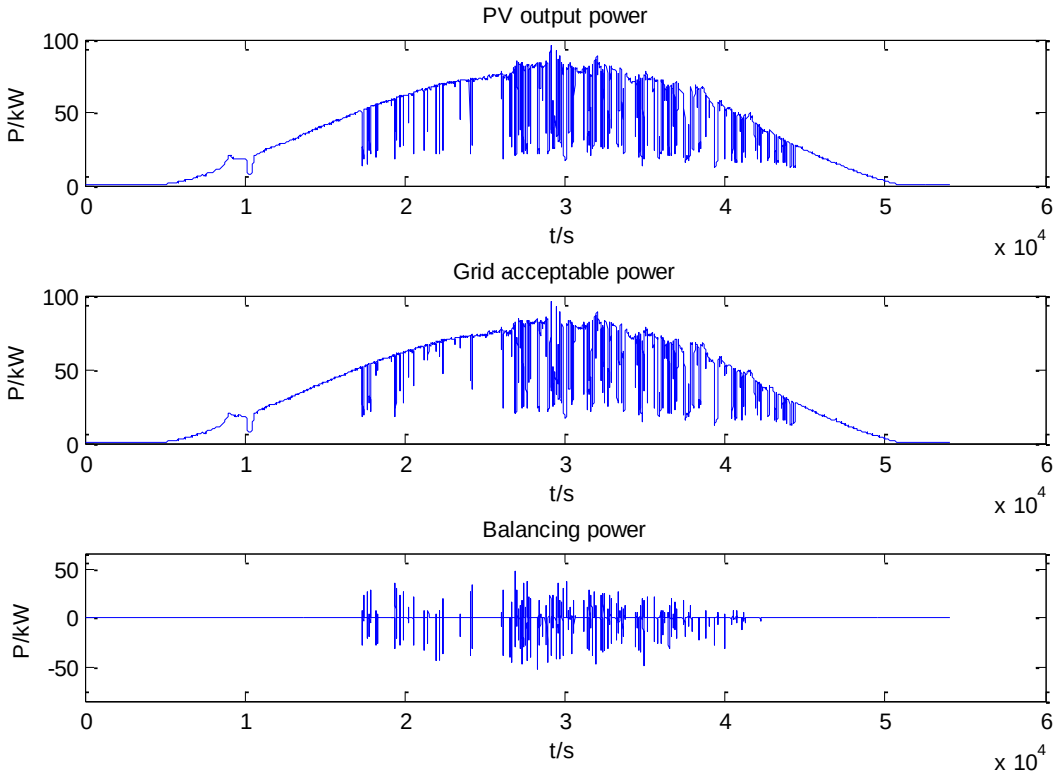

Figure 2-7 Balancing power

2.4 Case Selection

Based on sampling data which is recorded every seconds (sampling frequency: 1Hz) between 5:00 a.m. and 8:00 p.m. (54001 data per day) in 2015, Milwaukee, the weather in a year can be divided into 5 types: sunny, cloudy, overcast, rainy, and snowy. Typical light illumination curve under each weather are shown in Figure 2-8.

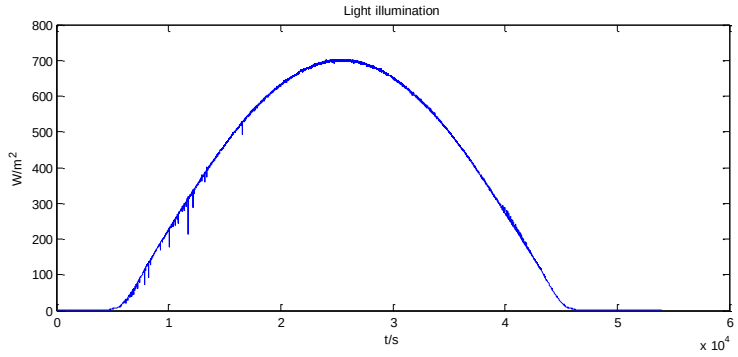

(1) Sunny

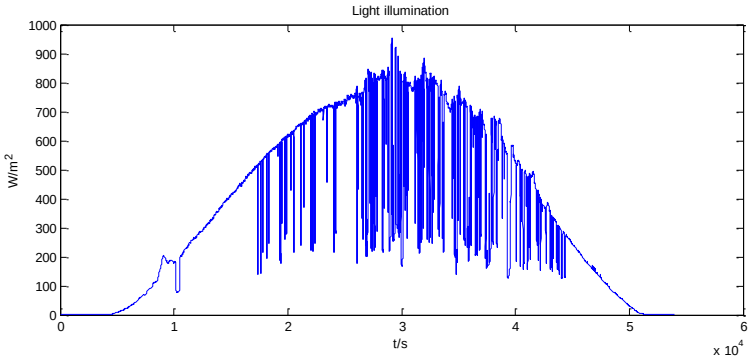

(2) Cloudy

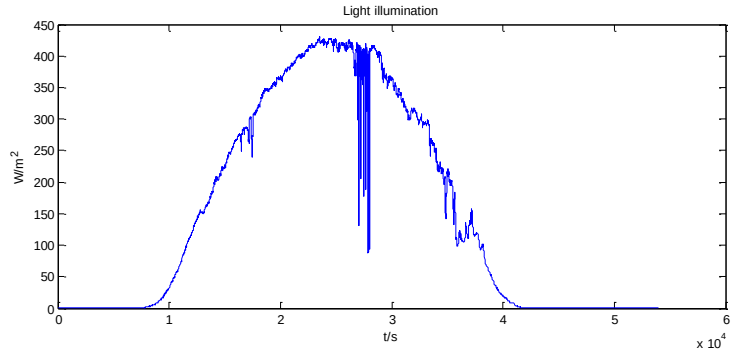

(3) Overcast

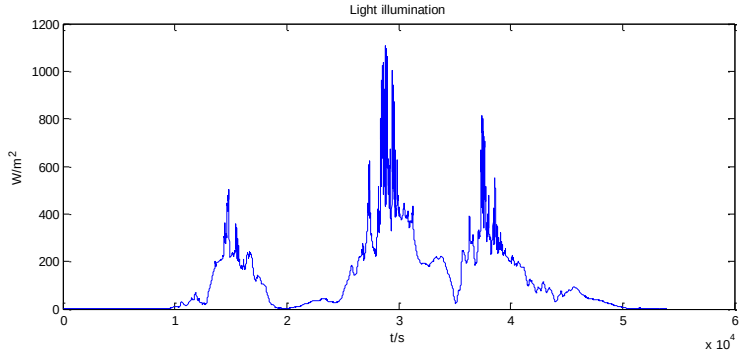

(4) Rainy

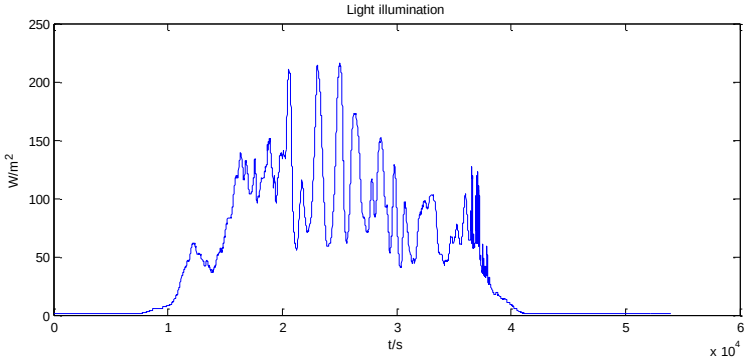

(5) Snowy

Figure 2-8 Typical light illumination curve under each weather

It can be seen from these curves that light illumination has the largest fluctuation in cloudy days. That's because under this weather, light illumination itself is stronger than overcast, rainy or

snowy days. Because of the existence of clouds, light cannot always reach PV panel directly, thus large fluctuations will happen.

Based on this theory, worst case is selected to design the ESS. First, 14 cloudy days are all selected between July 1st to September 30th in 2015. In this period, light illumination is the strongest in all year. Balancing power of each case is calculated according to chapters 2.3 before. Then balancing energy can be obtained by conducting integration. The maximum balancing power and maximum balancing energy in each case are recorded as in Figure 2-9.

Figure 2-9 Maximum balancing power and maximum balancing energy in each case

As it can be seen in Figure 2-9, the 7th case, which is in September 1st, has both maximum power value and maximum energy value among all 14 cases. Thus in this research, we assume this case is the worst case in 2015.

2.5 FFT Method

A fast Fourier transform (FFT) algorithm computes the discrete Fourier transform (DFT) of a sequence, or its inverse. Fourier analysis converts a signal from its original domain (often time or space) to a representation in the frequency domain and vice versa. An FFT rapidly computes such transformations by factorizing the DFT matrix into a product of sparse (mostly zero) factors [23]. As a result, it manages to reduce the complexity of computing the DFT.

Different energy storage technologies are suited for operation over different time periods. The balancing power, as shown in Fig. 2-10 can be broken down into the components spanning different frequency ranges. This decomposition can be achieved by using FFT. Each component of the periodic signal, except for the zero frequency component, represents cycling energy that averages to zero over each cycle. [6]

Analysis equation (fast Fourier transform):

$$X[f] = \sum_{t=0}^{N-1} x[t] W_N^{tf}, f = 0, \dots, N-1 \quad (2\text{-}3)$$

Synthesis equation (inverse Fourier transform):

$$x[t] = \frac{1}{N} \sum_{f=0}^{N-1} X[f] W_N^{-tf}, f = 0, \dots, N-1 \quad (2\text{-}4)$$

where *N* is the number of the data points in the sequence:

$$(x[0], x[1], \dots, x[N-1]) \quad (2\text{-}5)$$

$$W_N^{tf} = e^{-j(2\pi/N)tf} \quad (2\text{-}6)$$

FFT method is conducted to the balancing power in worst case to convert balancing power from time domain into frequency domain as shown in Figure 2-10.

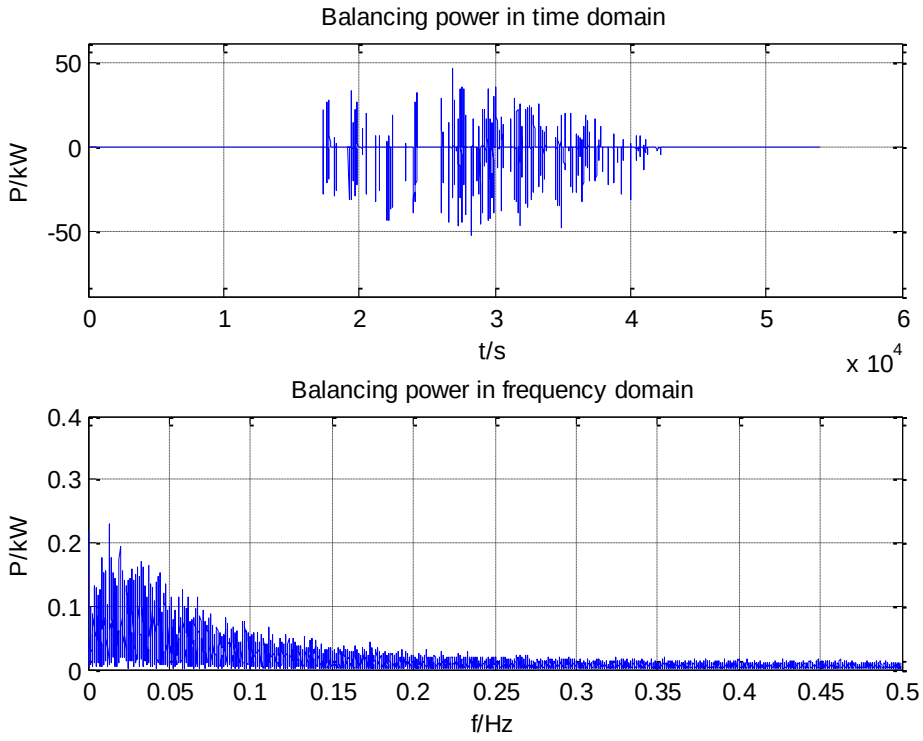

Figure 2-10 Balancing power after FFT

When the sampling interval is 1 second, balancing power is superposed by the set of power signals with different frequencies and amplitudes. The spectrum of the balancing power mainly concentrates on the low frequency band as shown in Fig. 2-10. The low frequency portion contains a DC component that corresponds to smooth and high amplitude signals. However, because of the existence of high frequency signals, even though their magnitudes are relatively low, when only use one ES in system, to smooth these high frequency signals, its power capacity needs to be oversized a lot, thus system total cost will increase.

The response rate of ES, such as the EDLC, is very fast and is well suitable for the compensation of the high frequency components. The power amplitudes of high frequency components are relatively low and will not lead to a high ES capacity.

Battery like lead acid and lithium ion have a relatively low response speed, thus the low frequency band is suitable for it. Therefore, it could track power variations, ranging from minutes to several hours.

Chapter 3 Energy Storage System Design

This section covers both the power and energy capacity calculation of ESS under different certain cutoff points to introduce sizing method. Later in chapter 4, to optimize the design, these cutoff points are adjusted.

3.1 Total Capacity Requirement

This section covers the entire system capacity of both power and energy calculation.

3.1.1 Total Power Capacity

Since real time powers in different frequency ranges will cumulate or offset by each other, the total power capacity has no practical significance. However, the power capacity is important

when calculating the total cost of each ES. Since each ES has to meet the requirement of both power capacity and energy capacity, and for each one ES, the ratio of its rated energy capacity and rated power capacity is a constant value. When ES power capacity is determined and its corresponding energy capacity is much larger than required, or if corresponding power capacity is much larger than required, the cost will be relatively high because of the oversizing. For these reasons, power capacities of each battery should be average and small to lower the total cost. This goal will be realized in the optimization chapter by adjusting cutoff point, which is to divide the smoothing frequency band of long-term ES and short-term ES.

3.1.2 Total Energy Capacity

Total energy curve can be calculated by integrating the balancing power as shown in Fig. 3-1, thus the minimum total energy requirement capacity equals to the maximum absolute peak value (maximum value or minimum value, depends on which absolute value is greater) which equals to 1.62kWh in this case.

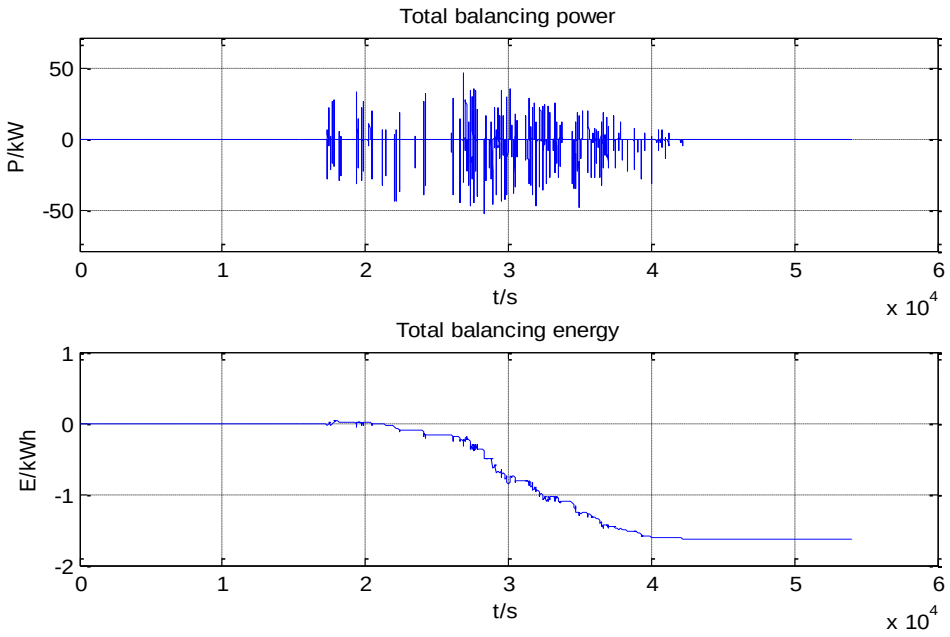

Figure 3-1 Total balancing power and energy

After the energy capacity of each ES is determined, we need to make sure that after adding all of them together, the total value is no less than the minimum total energy requirement capacity obtained here. That means when adding energy capacities of long-term ES and short-term ES together, the total capacity should not be less than energy capacity when only use one ES in the system.

3.1.3 Energy Capacity Considering State of Charge

State of charge (SOC) is the equivalent of a fuel gauge for the battery pack in a battery electric vehicle (BEV), hybrid vehicle (HV), or plug-in hybrid electric vehicle (PHEV). The units of SOC are percentage points (0% = empty; 100% = full). An alternate form of the same measure is the depth of discharge (DoD), the inverse of SOC (100% = empty; 0% = full). SOC is normally

used when discussing the current state of a battery in use, while DoD is most often seen when discussing the lifetime of the battery after repeated use. [24]

Taking SOC factor into consideration, to ensure that daily energy can always meet the requirement of power grid, no matter charging or discharging, we assume the PV system will go back to 50% SOC (to charge or to discharge are of the same possibility) every morning at 5:00am after all night control adjustment.

Thus the energy capacity of each battery should be 2 times of the calculated energy capacity, which is 1.62kWh. Thus the total balancing energy capacity is 3.24kWh in this case.

3.2 Cutoff points and ESS types

Based on response time of each battery, combined with data in reference, three kinds of ESS, which are commonly used: lead acid battery, lithium ion battery and EDLC are researched according to literature[25], [26] and[27].

Table 3-1 ESS type

ESS	Type	Shortest response time	Maximum response frequency
lead acid battery	long-term	2min	8.33×10^{-3}Hz
lithium ion battery	long-term	1min	0.0167Hz
EDLC	short-term	1s	1.00Hz

Based on Nyquist–Shannon sampling theorem, Sampling is the process of converting a signal (for example, a function of continuous time and/or space) into a numeric sequence (a function of discrete time and/or space). Shannon's version of the theorem states:[28]

If a function x(t) contains no frequencies higher than B hertz, it is completely determined by giving its ordinates at a series of points spaced 1/(2B) seconds apart.

In another words, signal function x(t) must contain no sinusoidal component at exactly frequency B, or that B must be strictly less than ½ the sample rate. sample–rate in this case is 1sample/second, thus its Nyquist frequency is 0.5Hz. Which means, the total frequency range by adding each battery frequency together should cover [0,0.5] Hz. Frequency band each ESS can cover is shown in Figure 3-2.

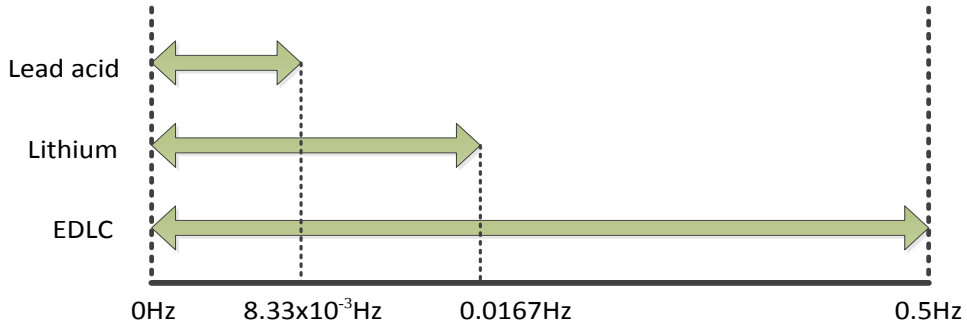

Figure 3-2 Frequency band each ESS can cover

As shown in a hybrid ESS, since lead acid battery and lithium battery cannot cover the high frequency band, EDLC have to exist. Obviously, the energy system only contain EDLC will cost much higher than hybrid one, thus two kinds of hybrid ESS are researched in this chapter: lead

acid battery with EDLC and lithium battery with EDLC. In this chapter, cutoff points are set as 8.33×10^{-3}Hz and 0.0167Hz respectively.

3.3 Lead Acid Battery with EDLC System

Combination and cutoff point of hybrid ESS with lead acid battery and EDLC are shown in Figure 3-3.

Figure 3-3 Combination and cutoff point of lead acid battery and EDLC

Actually, cutoff point can move from 0Hz to 8.33×10^{-3}Hz, this will be discussed in chapter 4 later. Here we use the maximum frequency value long-term ES can response as the constant cutoff point, which is 8.33×10^{-3}Hz.

3.3.1 ESS Power Capacity

Then FFT filtering can be conducted by keeping the frequency we need and setting the other one as zero. As shown in Figure 3-4, for lead acid battery, a low pass filter can be set to clean the power within [8.33×10^{-3}Hz, 0.5Hz] while keep the power within [0Hz, 8.33×10^{-3}Hz]. For EDLC, a high pass filter can be set to clean the power within [0Hz, 8.33×10^{-3}Hz] while keep the power left.

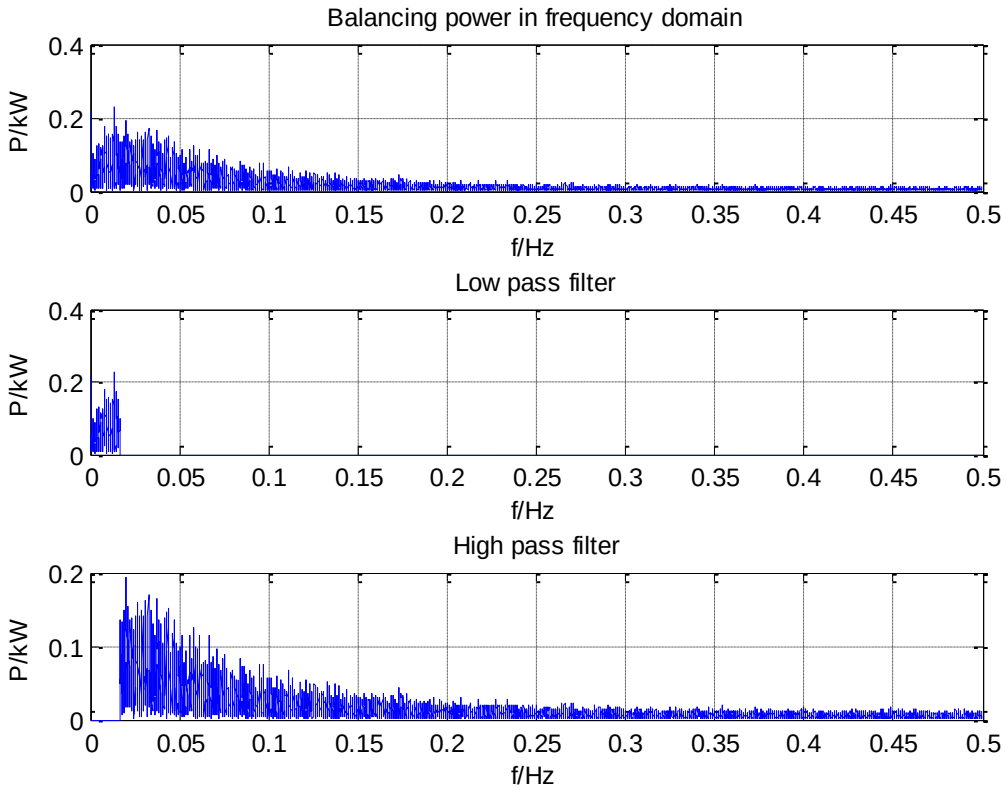

Figure 3-4 Balancing power after low pass filtering and high pass filtering

Then covert the function after filtering into time domain by conducting inverse FFT (iFFT) with only one certain frequency power as show in Figure 3-5. There may be some phase shift in each frequency after iFFT, but the average value after adding them together will be of less mismatch which can be neglected.

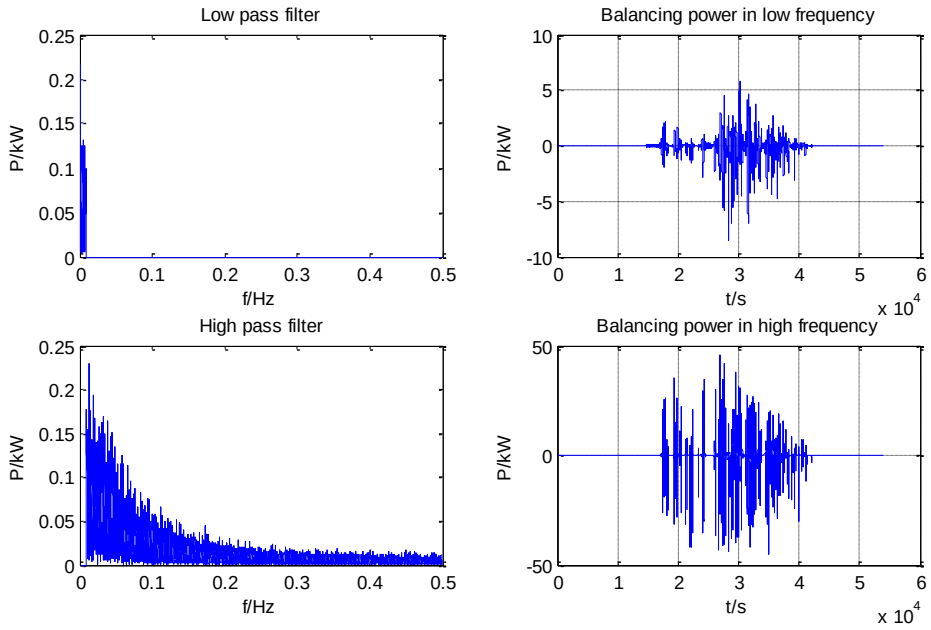

Figure 3-5 Balancing power in each frequency after iFFT

It can be seen in the result that more balancing powers that need to be take care by ESS is in high frequency, which means the power capacity of EDLC will be relatively larger than lead acid.

To cover all the power fluctuation, the power capacity of each ES is determined based on the peak value (maximum or minimum) in time domain of certain frequency:

- Lead acid battery: 8.52kW
- EDLC: 45.90kW

3.3.2 ESS Energy Capacity

Integration of balancing power in different frequency band can be conducted to calculate the energy capacity of each battery with certain frequency as shown in Figure 3-6.

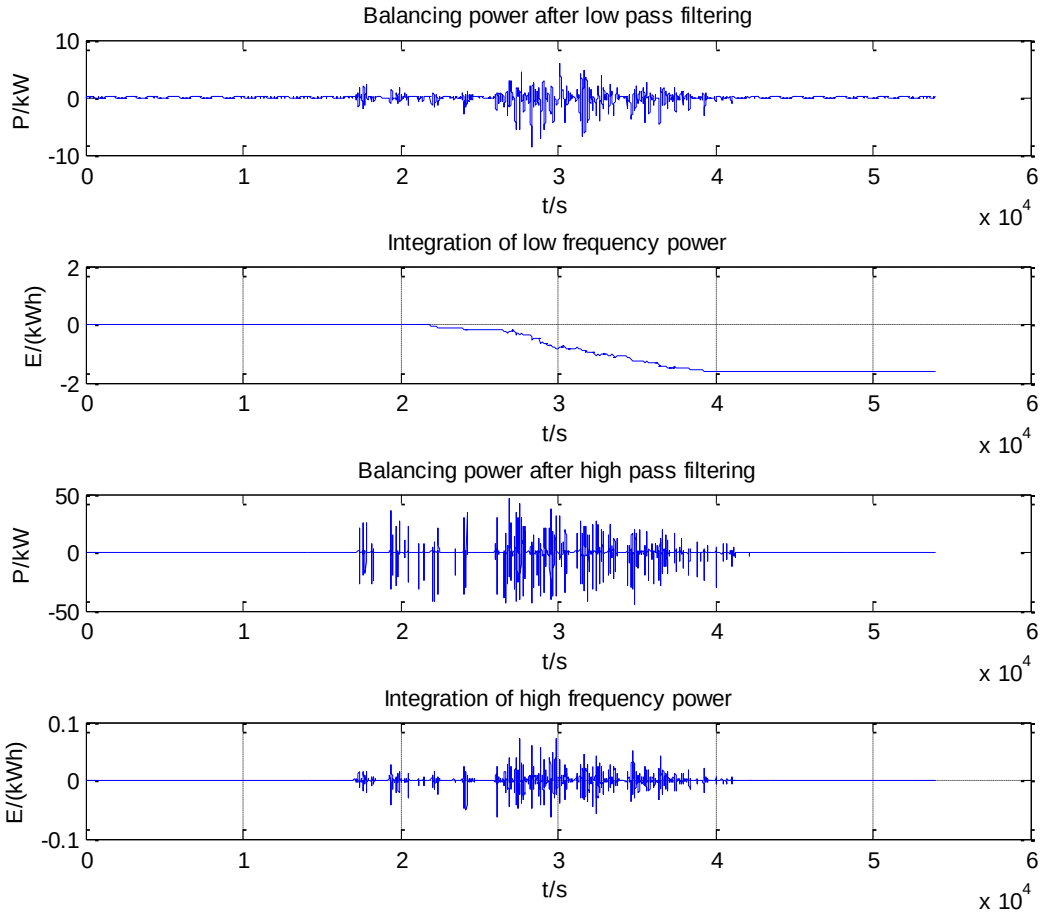

Figure 3-6 Balancing power in each frequency after integration

Thus the energy capacity can be obtained as the peak value in energy curve, considering 50% SOC:

- Lead acid battery: 3.24kWh
- EDLC: 0.14kWh

It can be seen that lead acid energy capacity is relatively larger than EDLC energy capacity.

3.4 Lithium Battery with EDLC System

Combination and cutoff point of hybrid ESS with lithium battery and EDLC are shown in Figure 3-7.

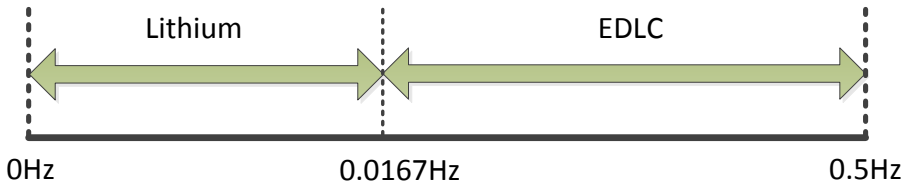

Figure 3-7 Combination and cutoff point of lead acid battery and EDLC

Same as before, cutoff point can move from 0Hz to 0.0167Hz. Here we use the maximum frequency value long-term ES can response as the constant cutoff point, which is 0.0167Hz.

3.4.1 ESS Power Capacity

For lithium battery, a low pass filter can be set to clean the power within [0.0167Hz, 0.5Hz] while keep the power within [0Hz, 0.0167Hz]. For EDLC, a high pass filter can be set to clean the power within [0Hz, 0.0167Hz] while keep the power left.

Then covert the function after filtering into time domain by conducting inverse FFT (iFFT) with only one certain frequency power as show in Figure 3-8.

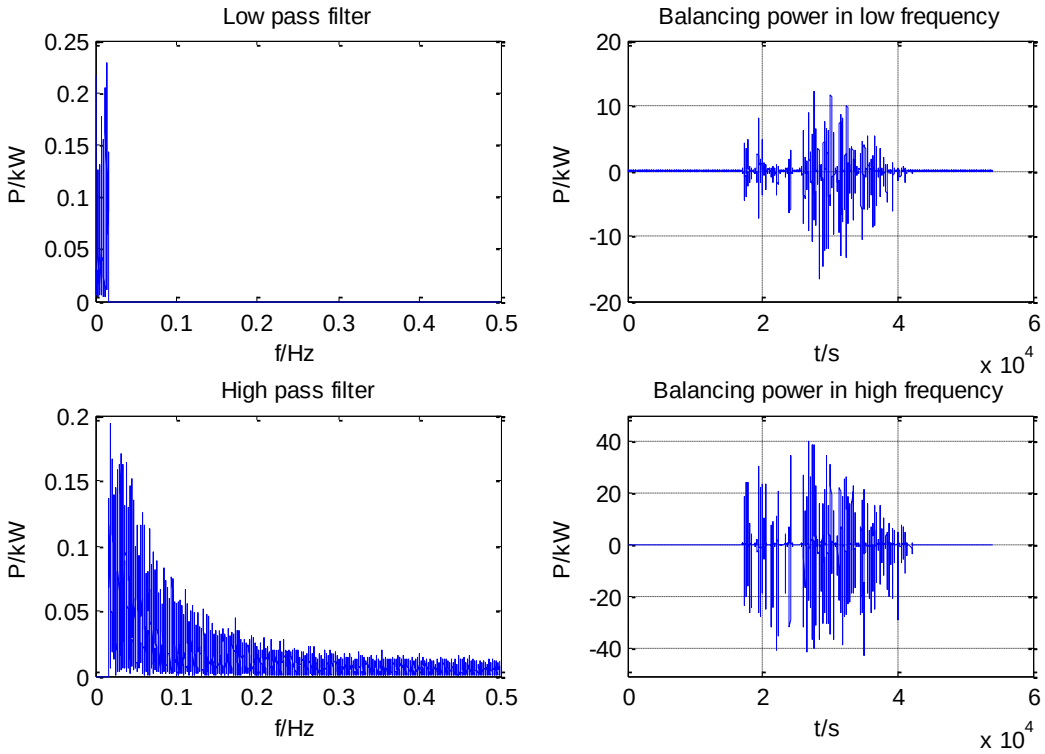

Figure 3-8 Balancing power in each frequency after iFFT

To cover all the power fluctuation, the power capacity of each ES is determined based on the peak value (maximum or minimum) in time domain of certain frequency:

- Lead acid battery：16.64kW
- EDLC：42.19kW

3.4.2 ESS Energy Capacity

Integration of balancing power in different frequency band can be conducted to calculate the energy capacity of each battery with certain frequency as shown in Figure 3-9.

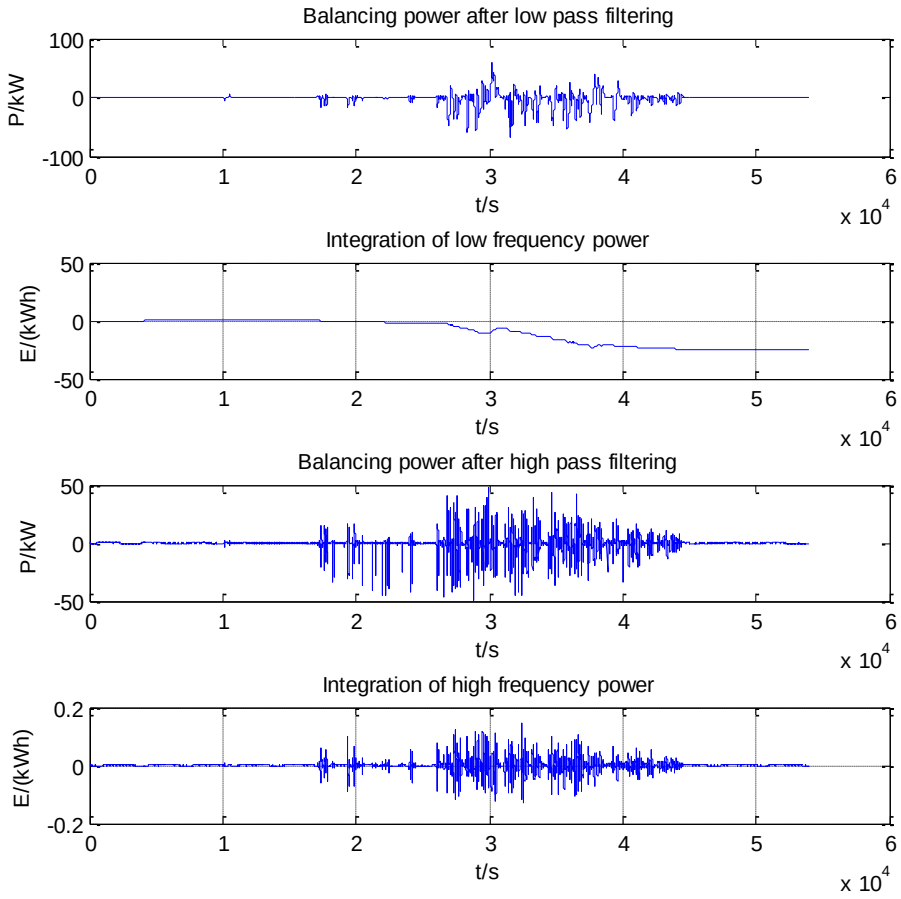

Figure 3-9 Balancing power in each frequency after integration

Thus the energy capacity can be obtained as the peak value in energy curve, considering 50% SOC:

- Lithium battery: 3.24kWh
- EDLC: 0.10kWh

It can be seen that the energy capacity of lithium battery is much larger than EDLC energy capacity.

Chapter 4 Cost Optimization

In chapter 3, to simplify the algorithm, we assume that there's only one certain cutoff point in each ES combination. The certain cutoff point is of high chance that not the optimal one. And we assume that each ES cycle life is infinite, which means they don't need to change, thus all the costs are one-time costs. However, since PV station has its own operation length, battery with short cycle life usually needs to be replaced several times before PV station being abandoned. Also, battery charge/discharge loss is neglected in chapter 3, which may cause calculated capacities relatively smaller than actual required capacities. In the end of this chapter, 3 ES are combined together to smooth the PV fluctuation. Results of the combination of 3 ES and 2 ES are compared and analyzed.

Taking all these facts into consideration, ESS costs are no longer the same as we calculated in the last chapter. In order to make this sizing method more practical and more effective, these factors will be discussed in this chapter.

4.1 System Cost

Based on literature [25], [29] and [30], unit costs of power, energy, cycle life, and ratios of E/p are list in Table 4-1 below.

Table 4-1 ESS information

Battery type	Unit cost		Cycle life	Cost ratio
	P ($/kW)	E ($/kWh)	(times)	(P/E)
Lead acid	200	100	1000	2
Lithium	500	300	2000	5/3
EDLC	150	4000	100000	3/80

The cost of the storage unit[31]:

$$Battery\ energy\ cost\ (\$) = Unit\ Coststorage(\$/kWh) \times E(kWh) \tag{4-1}$$

$$Battery\ power\ cost\ (\$) = Unit\ Coststorage(\$/kW) \times P(kW) \tag{4-2}$$

Where, *E(kWh)* and *P(kW)* represent rated energy and power capacities of a battery.

Since for certain ES in the market,

$$Battery\ energy\ cost\ (\$) = Battery\ power\ cost\ (\$) \tag{4-3}$$

Which means,

$$Unit\ Coststorage(\$/kWh) \times E(kWh) = Unit\ Coststorage(\$/kW) \times P(kW) \tag{4-4}$$

$$\frac{E(kWh)}{P(kW)} = \frac{Unit\ Coststorage(\$/kW)}{Unit\ Coststorage(\$/kWh)} = cost\ ratio \tag{4-5}$$

In this paper, when not taking cycle life and battery loss into consideration, system total cost is calculated as the greater one between total power cost and total energy cost to make sure that battery can meet both requirements of energy capacity and power capacity.

Suppose *Total energy cost* and *Total power cost* are total costs calculated by resulted power and energy capacity. If

$$Total\ energy\ cost\ (\$) > Total\ power\ cost\ (\$) \tag{4-6}$$

ESS actual power capacity should be oversized to meet energy capacity requirement. In this case, the actual ES power capacity is no longer the calculated value, it becomes

$$Actual\ power\ capacity = \frac{Calculated\ energy\ capacity}{cost\ ratio} \tag{4-7}$$

If

$$Total\ energy\ cost\ (\$) < Total\ power\ cost\ (\$) \tag{4-8}$$

ESS actual energy capacity should be oversized to meet power capacity requirement. In this case, the actual ES energy capacity is no longer the calculated value, it becomes

$$Actual\ energy\ capacity = Calculated\ power\ capacity \times cost\ ratio \tag{4-9}$$

Based on this, energy storage capacities of both power and energy and their corresponding costs under different combinations are listed in Table 4-2 and Table 4-3.

Table 4-2 Lead acid battery+EDLC with cutoff point at 2min

cutoff point: 2min	Calculated capacity		Calculated cost		Actual capacity		Actual Cost ($)
	P (kW)	E (kWh)	P ($)	E ($)	P (kW)	E (kWh)	
Lead acid	8.52	3.24	1704	324	8.52	17.04	1740
EDLC	45.90	0.14	6885	560	45.90	1.72	6880
Total							8620

Table 4-3 Lithium battery+EDLC with cutoff point at 1min

cutoff point: 1min	Calculated capacity		Calculated cost		Actual capacity		Actual Cost ($)
	P (kW)	E (kWh)	P ($)	E ($)	P (kW)	E (kWh)	
Lithium	16.64	3.24	8320	972	16.64	27.73	8320
EDLC	42.19	0.1	6328.5	400	42.19	1.58	6328.5
Total							14648.5

4.2 Cost under different cutoff points

In Chapter 3, cutoff points are set as a constant highest frequency value which long-term ES can cover in frequency domain. However, in practical design, cutoff points can move between 0Hz to the highest frequency. Cost of short-term ES and long-term ES will change under different cutoff points. Thus ESS total cost will also change.

In the combination of lead acid with EDLC, cutoff point can move between [0, 8.33×10^{-3}] Hz. In the combination of lithium with EDLC, cutoff point can move between [0, 0.0167] Hz.

In order to find the minimum total cost value and its corresponding ES capacity, first, ES capacity of both power and energy under different cutoff points are obtained as shown in Figure 4-1 below.

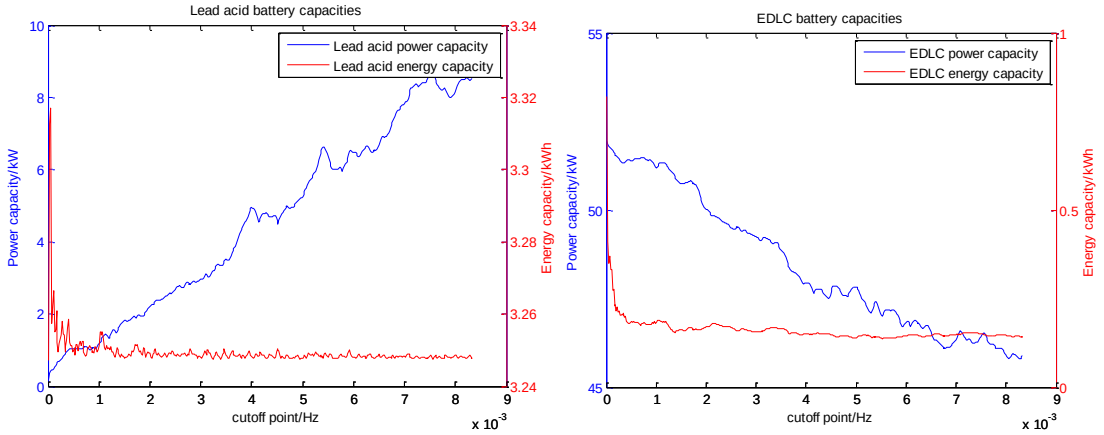

(1) lead acid battery+EDLC

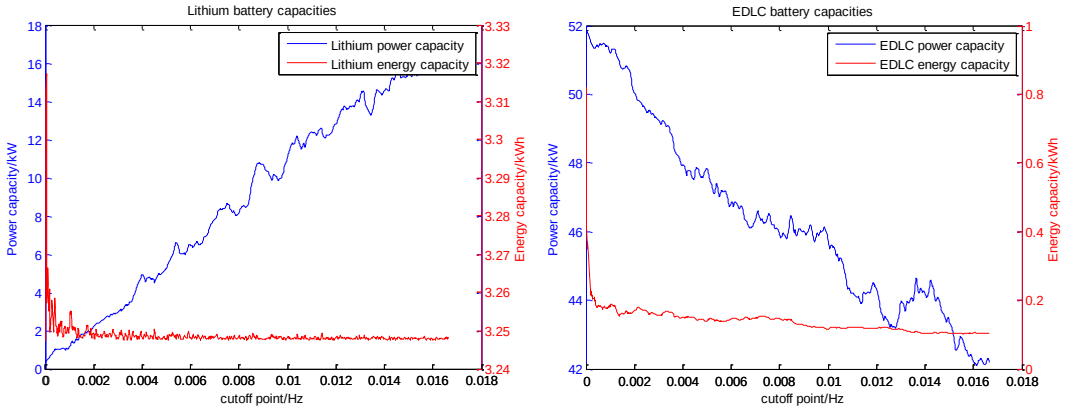

(2) lithium battery+EDLC

Figure 4-1 ES capacities under different cutoff points

Thus ESS total costs under different cutoff points can be calculated. Their tendency curves are shown in Figure 4-2, where blue line is the power capacity of each ES, red line is the energy capacity of each ES. With the cutoff point moving towards right, the requirement for long-term ES increase, and requirement for short-term ES decrease. That's why the blue lines in the left figures go up, and in the right figures go down. Since in this case, the energy capacities will not change greatly when cutoff points changed. Thus the value of red line can be seen as a constant. Because of the error in algorithm, at the beginning of frequency range, red line fluctuates a little bit. But since that fluctuation is relatively small, it won't affect the final results.

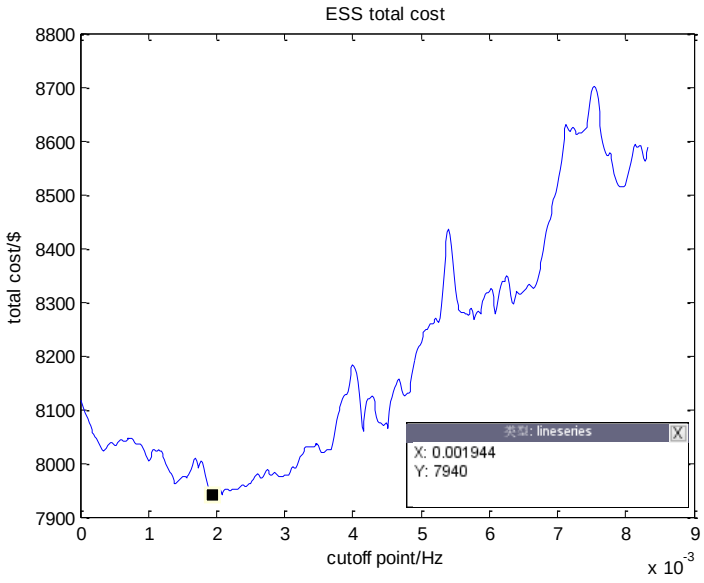

(1) lead acid battery+EDLC

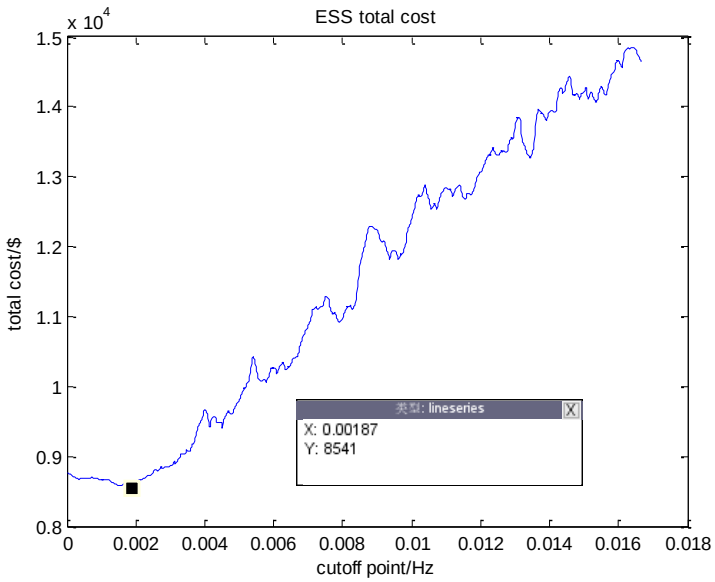

(2) lithium battery+EDLC

Figure 4-2 ESS total costs under different cutoff points

When cutoff point moving within the long-term ES response frequency range, the power capacities and energy capacities of each ES will change, thus system total cost won't stay the same value. According to the results, minimum total costs under different combinations are listed in Table 4-4 below:

Table 4-4 ESS calculated capacities

Cutoff point/Hz	**Lead acid**		**Lithium**		**EDLC**		**Minimum cost/$**
	P/kW	E/kWh	P/kW	E/kWh	P/kW	E/kWh	
0.001944	2.10	3.25			50.14	0.17	7940
0.001870			1.95	3.25	50.44	0.16	8541

According to algorithm in chapter 4.1, ES power capacities and energy capacities are modified based on parameters of battery on the market to meet both requirements. Practical capacities after modification are listed in Table 4-5.

Table 4-5 ESS practical capacities

Cutoff point/Hz	Lead acid		Lithium		EDLC		Minimum cost/$
	P/kW	E/kWh	P/kW	E/kWh	P/kW	E/kWh	
0.001944	2.10	4.20			50.14	1.88	7940
0.001870			1.95	3.25	50.44	1.89	8541

It can be seen in this table that the combination of lead acid battery and EDLC is of the lowest cost in both combinations, which is $7940. Thus when not consider cycle life and loss, the best ES combination and ES sizes are:

- Lead acid battery: 2.1kW, 4.2kWh
- EDLC: 50.14kW, 1.88kWh

4.3 Consider Cycle Life

Cycle life is a term used to specify a battery's expected life. In general, number of cycles for a rechargeable battery indicates how many times it can undergo the process of complete charging and discharging until failure or it starting to lose capacity [32].

Assume designed PV station will operate for 15 years. Thus the battery change time can be calculated as equation below assuming no loss in charging and discharging process.

$$battery\ \ change\ \ time = \frac{PV\ \ station\ \ total\ \ requirement\ \ in\ \ 15\ \ years}{total\ \ energy\ \ battery\ \ can\ \ provide} \quad (4\text{-}10)$$

4.3.1 PV Station Total Requirement

Using one-day maximum charging or discharging total value under the worst case in certain frequency multiply by number of days in 15 years, which is 547 to simplify the calculation of PV total requirement.

To obtain the one-day maximum charging or discharging power in certain frequency, after FFT filtering and converting into time domain, positive power and negative power are integrated respectively. Positive value represents ESS discharging power and negative value represents ESS charging power. After conducting integration, the final value of positive and negative integration represents ESS discharging and charging energies. The greater one of these two integration results are selected as the one-day maximum charging or discharging total value in this frequency band. The flow chart of calculation is shown in Figure 4-3.

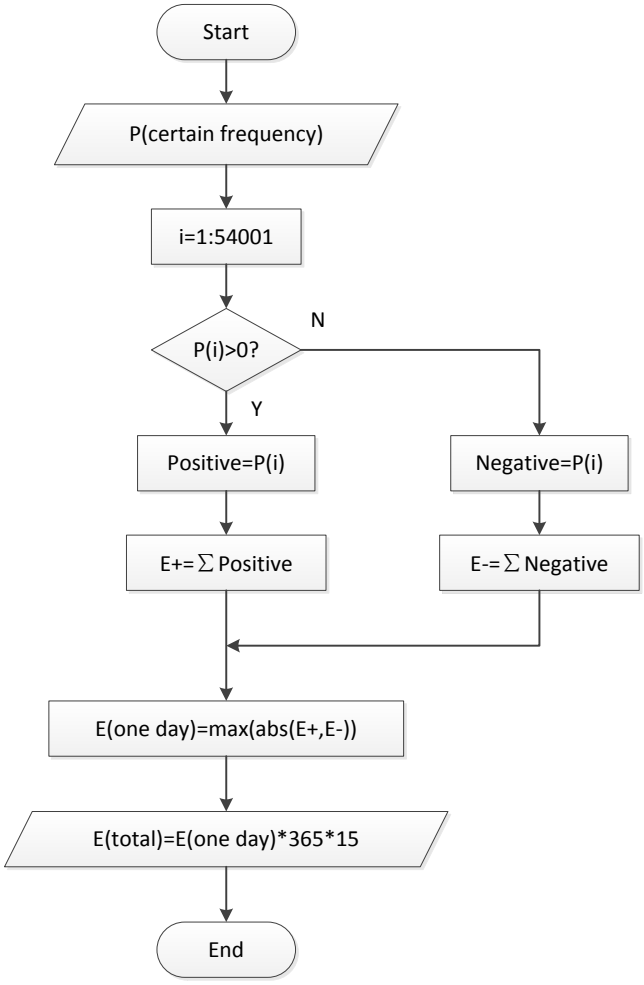

Figure 4-1 Flow chart of one-day maximum charging/ discharging total value

4.3.2 Total Energy Battery Can Provide

Energy battery can provide in its cycle life is calculated as below:

$$total\ \ energy = battery\ \ practical\, capacity/2 \times cyclelife \tag{4-11}$$

According to chapter 4.1, battery practical capacity is the energy capacity calculated based on practical battery parameters, it isn't always equal to the calculated energy capacity. Since ES

SOC is set as 50%, real energy battery can constantly charge or discharge is half of its total practical capacity. Flow chart of total energy calculation is shown in Figure 4-4.

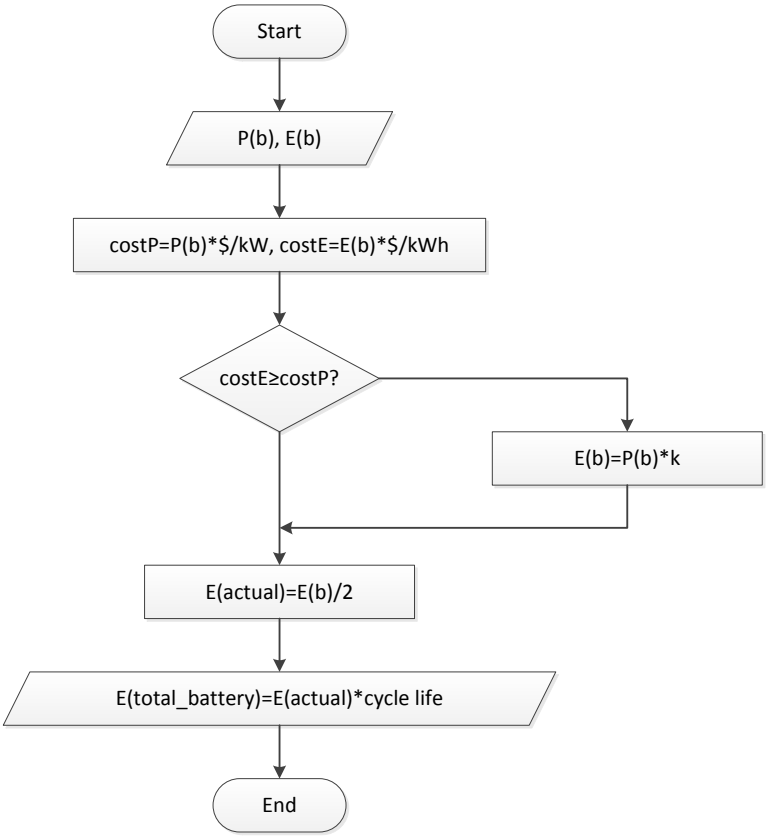

Figure 4-2 Flow chart of total energy calculation

Where, *k* is the cost ratio mentioned and calculated in chapter 3.

4.3.3 Battery replacement and Total Cost

The number of needed replacement for each battery can be calculated by the outputs in both algorithm:

$$battery\ \ replacement\ \ times = \frac{E(total)}{E(total\_battery)} \tag{4-12}$$

Thus Battery replacement times under different combinations can be calculated as shown in Figure 4-5 below.

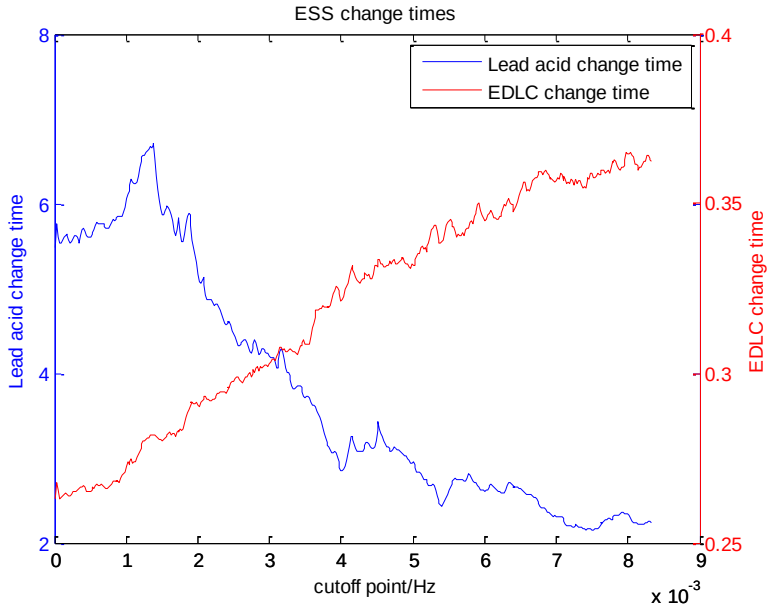

(1) Lead acid battery+EDLC

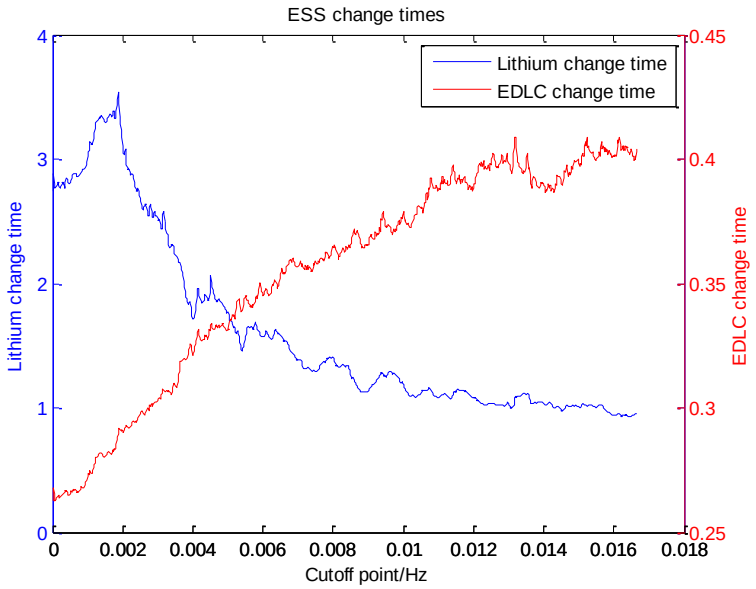

(2) Lithium battery+EDLC

Figure 4-3 Battery change times under different combinations

It can be seen that change times of EDLC in both combinations are always much smaller than 1, which means it doesn't need replacement. To be more practical, here we set EDLC change time as constant 1 when calculating EDLC total cost. After considering battery cycle life, ESS total cost can be calculated:

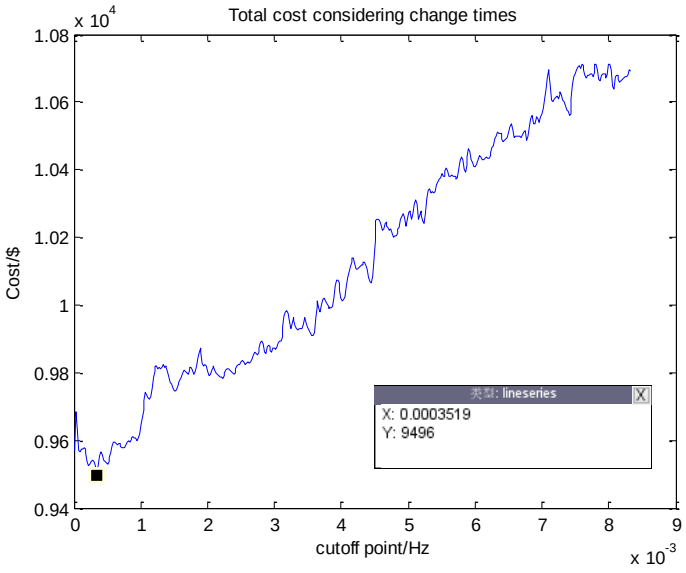

(1) Lead acid battery+EDLC

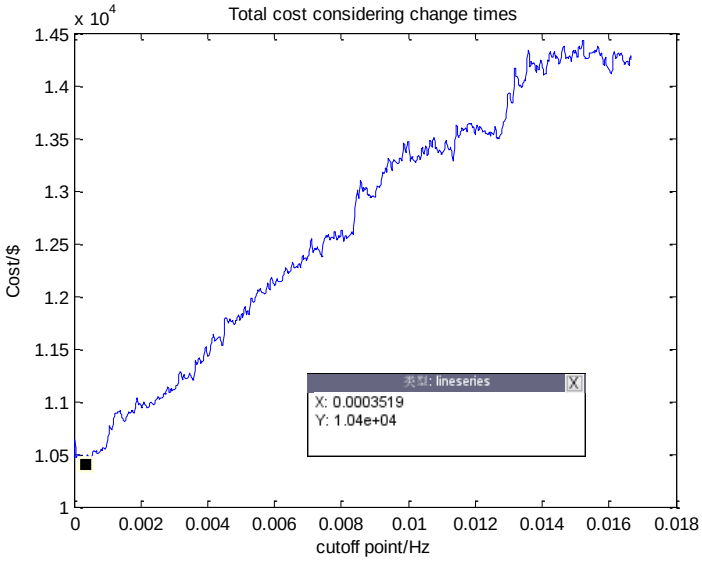

(2) Lithium battery+EDLC

Figure 4-4 ESS total cost

Minimum total cost under different combinations when taking cycle life into consideration are listed in table below:

Table 4-6 Lead acid+EDLC combination

Cutoff point/Hz	Lead acid		Change time	EDLC		Minimum cost/$
	P/kW	E/kWh		P/kW	E/kWh	
0.0003519	0.93	3.25	5.53	51.32	0.21	9463

Table 4-7 Lithium+EDLC combination

Cutoff point/Hz	Lithium		Change time	EDLC		Minimum cost/$
	P/kW	E/kWh		P/kW	E/kWh	
0.0003519	0.93	3.25	2.766	51.32	0.21	10396

It can be seen in this table that the combination of lead acid battery and EDLC is still of the lowest cost in both combinations, which is $9463. ES power capacities and energy capacities are modified based on parameters of battery on the market to meet both requirements. Practical capacities after modification are listed in Table 4-8.

Table 4-8 Best practical capacity combination

Cutoff point/Hz	Lead acid		Change time	EDLC		Minimum cost/$
	P/kW	E/kWh		P/kW	E/kWh	
0.0003519	1.63	3.25	5.53	51.32	1.92	9463

Thus the best combination and corresponding actual ES sizes are:

- Lead acid battery: 1.63kW, 3.25kWh
- EDLC: 51.32kW, 1.92kWh

4.4 Capacity Loss

Capacity loss or capacity fading is a phenomenon observed in rechargeable battery usage where the amount of charge a battery can deliver at the rated voltage decreases with use.[33][34]

In this paper, we assume that each ES will lose 40% capacity when reach its cycle life, which is the value of capacity loss for most ES, giving an average capacity loss per cycle *m* of:

- Lead acid battery: 4×10^{-4}
- Lithium battery: 2×10^{-4}
- EDLC: 4×10^{-6}

When taking loss into consideration, battery replacement time will change because of the difference of total provided energies. Based on chapter 4.3.2, flow chart of new total energy battery can provide calculation with loss is shown in Figure 4-7.

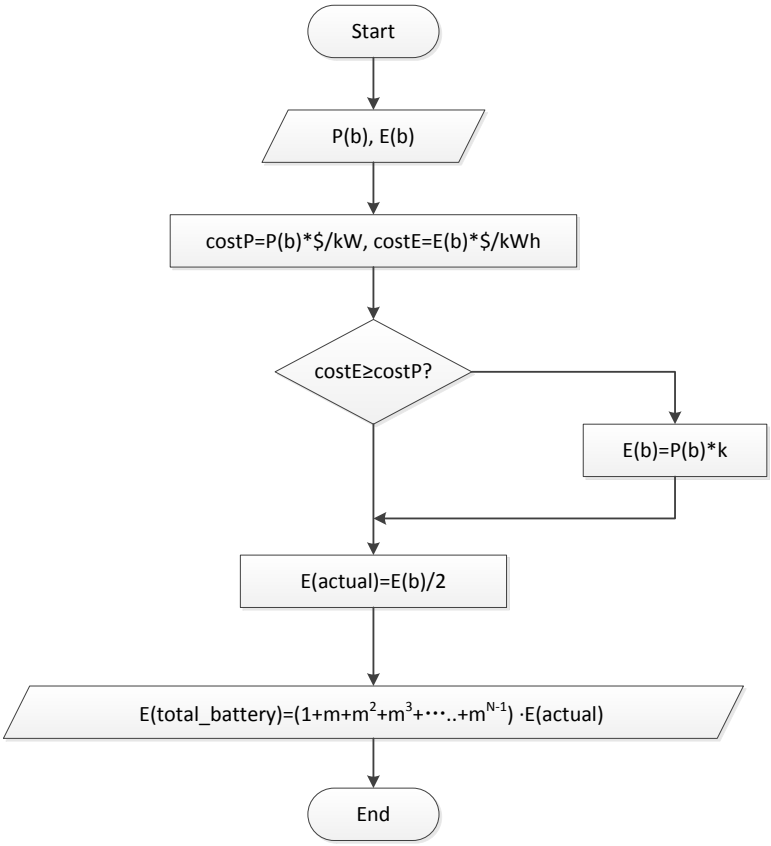

Figure 4-7 Flow chart of total energy calculation

Then battery change times and total cost can be obtained same as before. Results are shown in Figure 4-8 below. Since change times of EDLC are still much less than 1 after considering loss, here we assume change time of EDLC is 1 when calculating ESS total cost.

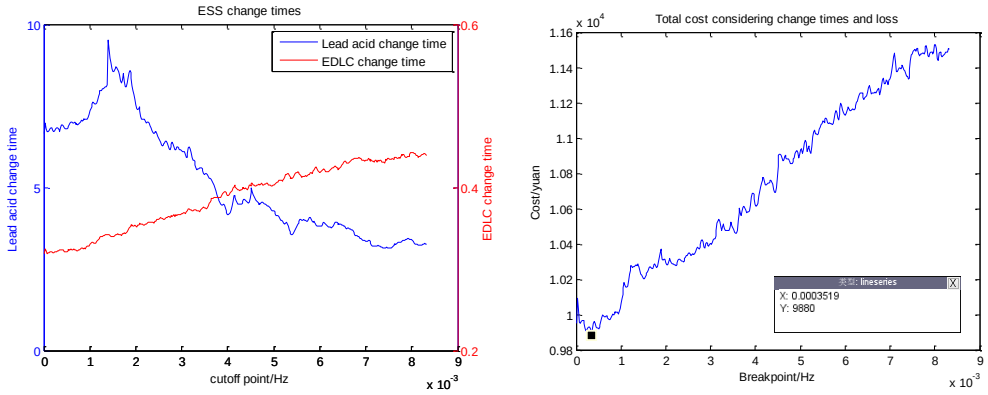

(1) Lead acid +EDLC

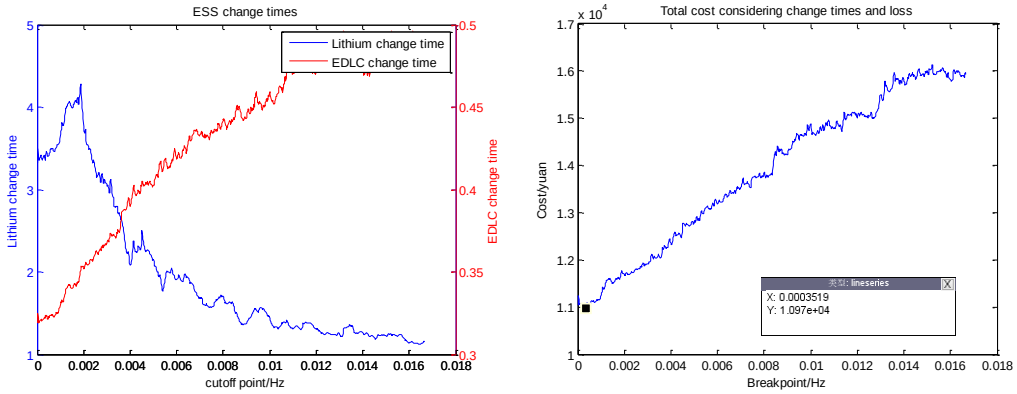

(2) Lithium +EDLC

Figure 4-8 ESS total cost

Minimum total cost under different combinations when taking loss into consideration are listed in table below:

Table 4-9 Lead acid+EDLC combination

Cutoff point/Hz	**Lead acid**		**Change time**	**EDLC**		**Minimum cost/$**
	P/kW	E/kWh		P/kW	E/kWh	
0.0003519	0.93	3.25	5.53	51.32	0.21	9880

Table 4-5 Lithium+EDLC combination

Cutoff point/Hz	**Lithium**		**Change time**	**EDLC**		**Minimum cost/$**
	P/kW	E/kWh		P/kW	E/kWh	
0.0003519	0.93	3.25	3.36	51.32	0.21	10971

It can be seen in this table that the combination of lead acid battery and EDLC is still of the lowest cost in both combinations, which is $9880. ES power capacities and energy capacities are modified based on parameters of battery on the market to meet both requirements. Practical capacities after modification are listed in Table 4-11.

Table 4-6 Best practical capacity combination

Cutoff point/Hz	Lead acid		Change time	EDLC		Minimum cost/$
	P/kW	E/kWh		P/kW	E/kWh	
0.0003519	1.63	3.25	5.53	51.32	1.92	9880

The only difference between only consider cycle life and consider both cycle life and loss is the change time of lead acid battery, thus total cost will increase a little bit. The best combination and corresponding actual ES sizes are same as in chapter 4.2.2:

- Lead acid battery: 1.63kW, 3.25kWh
- EDLC: 51.32kW, 1.92kWh

4.5 Three ESs

To further analyze ESS design and corresponding cost, lead acid battery, lithium battery and EDLC are combined together in one ESS. There are two cutoff points in this case. One is for dividing the cover frequency of lead acid batter and lithium battery, as we mentioned before, it can move between [0, 8.33×10^{-3}] Hz. The other one is for dividing the cover frequency of lithium battery and EDLC, this cutoff point can move between [0, 0.0167] Hz. These two cutoff points may coincide with each other, which means there's only one cutoff point (only two ES) in the system.

To simplify the coding program and save time, in this algorithm, cutoff point 1 is set moving between [0, 8.33×10^{-3}] Hz while the moving frequency range of cutoff point 2 is divided into

two part: [0, 8.33×10^{-3}] Hz and [8.33×10^{-3}, 0.0167] Hz. In the first part, we assume that cutoff point 2 cannot move beyond cutoff 1. System total under different cutoff points are calculated as shown in Figure 4-9.

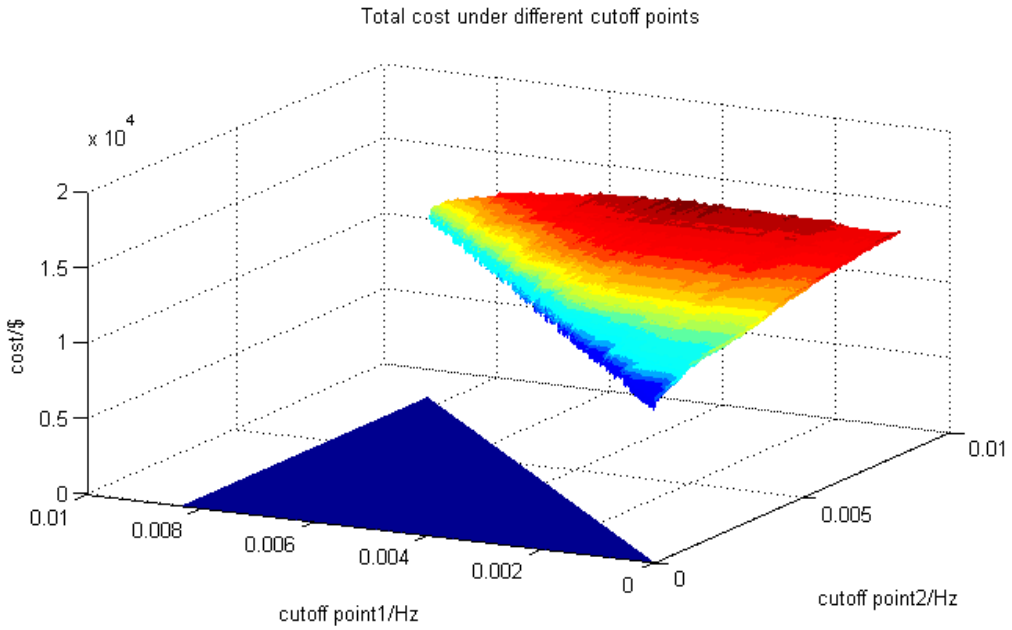

(1) Cutoff point 2 moves between [0, 8.33×10-3] Hz

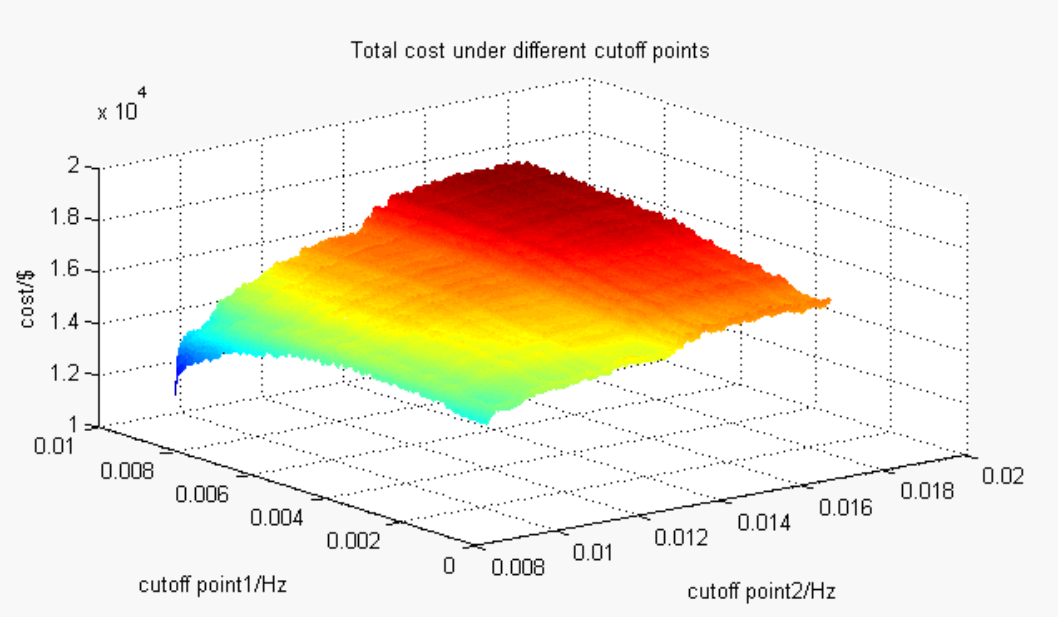

(2) Cutoff point 2 moves between [8.33×10-3, 0.0167] Hz

Figure 4-9 ESS cost under different cutoff points

From the first diagram when cutoff point moves between [0, 8.33×10-3] Hz, the minimum total cost of the system is $9880 when two cutoff points coincide with each other at 0.000352 Hz. And in the second diagram, the minimum total cost of the system is $\$1.15 \times 10^4$ when two cutoff points coincide with each other at 0.00833 Hz.

Apparently, the results show that system containing 2 ES cost lower than containing 3 ES. Thus the best design is still the same as in chapter 4.4:

- Lead acid battery: 1.63kW, 3.25kWh
- EDLC: 51.32kW, 1.92kWh

4.6 Summary

In this chapter, optimization of integrated ESS is conducted. The optimization object is to minimize system total cost. To achieve this goal, each cost is calculated when moving cutoff point from 0Hz to the maximum frequency long-term energy storage can take care. The minimum cost and its corresponding ESS capacities under all these frequencies is the optimal solution. All the optimal solution obtained in this chapter are listed in Table 4-12.

Table 4-12 Comparison of ESS design under different consideration

Consider Factor	Cutoff point/Hz	Lead acid		EDLC		Total cost/$
		P/kW	E/kWh	P/kW	E/kWh	
None	0.001944	2.1	4.2	50.14	1.88	7940
Cycle life	0.000352	1.63	3.25	51.32	1.92	9463
Capacity Loss	0.000352	1.63	3.25	51.32	1.92	9880

It can be seen that after considering cycle life, ESS total cost increase. Even though one EDLC can operate for 15 years without replacement, lithium battery and lead acid battery have to be replaced several times. After considering charging/discharging loss, ESS system total cost increase again. But the capacities of lead acid and EDLC, as well as the optimal cutoff point stay the same as when not considering loss. That's because the loss is relatively small, it won't affect the final result much in this case.

ESS with 3 ES is also researched. However, the results show that ESS with 3 ES cost higher than only 2 ES system. Thus the best design with lowest cost is the same as before.

Chapter 5 Verification

In order to make this design more reasonable and practical, which means this certain design is able to smooth PV output power fluctuation under all weathers, case verification is conducted in this chapter.

5.1 Better Case

Using the worst case results obtained in chapter 4.4 to conduct verification. Four kinds of better weather case mentioned in chapter 2 are applied to test if the optimal ESS obtained from the last chapter can adequately handle these different weather cases. The optimum ESS determined from the previous chapter was a lead acid and EDLC combination with the cutoff frequency of 0.0003519Hz. The power size for the lead acid battery is 1.63 kW and for the EDLC is 51.32 kW. The energy size for the lead acid battery is 3.25 kWh and for the EDLC is 1.92 kWh. The Results of comparison are listed in Table 5-1 below.

Table 5-1 Comparison of ESS design under different weather

Weather	**Lead acid**		**EDLC**	
	P/kW	E/kWh	P/kW	E/kWh
Cloudy (optimum design)	1.63	3.25	51.32	1.92
Sunny	0.01	0.01	7.59	0.28
Overcast	0.10	0.21	20.89	0.78
Rainy	0.22	0.45	34.27	1.29
Snowy	0	0	0	0

From this table, it can be seen that the fluctuation in snowy days can all be accepted by power grid, which means there's no need for ESS. In sunny, overcast and rainy weather, calculated ES capacities are all relatively smaller than in cloudy case, which is the selected worst case where the optimum design was based on.

Since cloudy weather is the selected worst case, its corresponding ES capacities should be larger than other better case, that means this certain ES design can meet the requirement of fluctuation smoothing in all weathers.

5.2 Worse Case

To further verify this proposed method, another cloudy-weather day data is selected. After data processing, most fluctuation values are amplified, thus makes this case even worse than the chosen case we used in chapters before. The corresponding PV output power, grid acceptable power, and balancing power are shown in Figure 5-1.

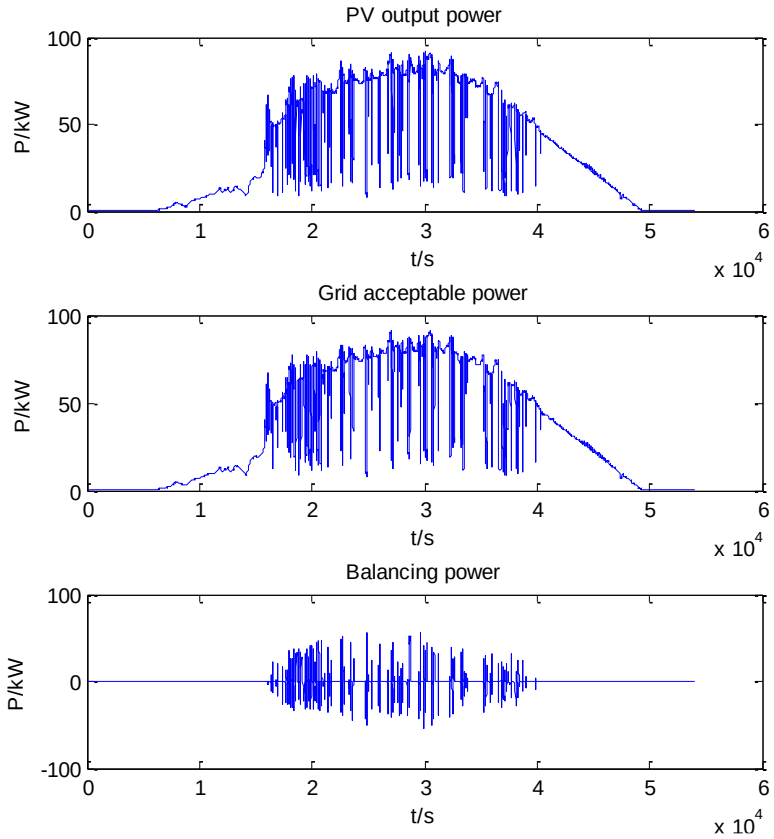

Figure 5-1 Balancing power of worse case

It can be seen that the peak power fluctuation value is greater than the original worst case. Thus the peak value of balancing power, which directly determines ES capacities, is larger than before.

Using the same algorithm, the best design of ESS under worse case considering both cycle life and loss is compared with the original worst case in Table 5-2.

Table 5-2 Comparison of ESS design between original case and worse case

Case	Lead acid		EDLC	
	P/kW	E/kWh	P/kW	E/kWh
Original	1.63	3.25	51.32	1.92
Worse	0.73	1.47	56.59	2.02

It can be seen from this table that both power and energy capacities of EDLC under worse case is greater than in the original case, which means that the original calculated ESS can no longer compensates the output power fluctuation under this worse weather.

5.2 Summary

In this chapter, case verification is conducted to make sure ES design in this research can meet the requirement of all other conditions, also to make sure selected worst case is a typical case. As the results prove, this design and optimization can cover all other cases. Calculated ESS capacities and combination are correct and reasonable.

Also, when weather become worse, the original design based on better case can no longer effectively smooth the fluctuation, which means the worst case is a key factor in ESS design.

Chapter 6 Conclusion and Future Work

6.1 Conclusion

According to the response characteristics of different energy storage equipment, a sizing method is proposed based on frequency analysis. A hybrid ESS including the combination of lead-acid battery, lithium ion battery and EDLC is applied to meet both power and energy smoothing requirement of the power grid. The FFT method is applied for analyzing the spectrum of balancing power, dividing the compensation frequency band for each type of storage equipment, and filtering. Then the power capacity and energy capacity of each energy storage equipment are determined by conducting inverse FFT within certain frequency range. After that, an optimization is conducted by considering ES cycle life, capacity loss during charging and discharging, and system contains three ESs together. Finally, several cases are used to verify the final optimal design.

The results show that, with the same smoothing requirement, system contains only two ESs has a lower total cost than system contains three ESs. And among all the ES combinations of two-ES

system, the combination of lead acid battery and EDLC has the minimum total cost. Also, the worst case selection directly determine the power and energy capacity of each ES.

6.2 Future Work

A practical Matlab/Simulink model of PV and ESS will be built using calculated capacities of ESS to conduct real time simulation. If the simulation demonstrates the selected hybrid ESS can effectively smooth the fluctuation in PV system, then it will prove the validity of this proposed method.

Also, more considerations, such as ESS control methods, ESS installation location, and ES response latency should be included in the optimization part to make the result more reasonable and practical.

Finally, in the worst case selection part, more weather and location should be considered. Statistic algorithm can be applied to define a specific worst case standard. This will also benefit the case verification work in chapter 5.

References

[1] IEA-PVPS, P. V. P. S. (2015). Report Snapshot of Global PV 1992-2014.Report IEA-PVPS T1-26.

[2] Hongxin J, Yang F, Yu Z, et al. Design of hybrid energy storage control system for wind farms based on flow battery and electric double-layer capacitor[C]//Power and Energy Engineering Conference (APPEEC), 2010 Asia-Pacific. IEEE, 2010: 1-6.

[3] J. C. Smith, M. R. Milligan, E. A. DeMeo, and B. Parsons, "Utility wind integration and operating impact state of the art," IEEE Trans. Power Syst., vol. 22, no. 3, pp. 900–908, Aug. 2007.

[4] A. Ter-Gazarian, Energy Storage for Power Systems. London: Peter Peregrinus, Sep. 1994, ISBN-10: 0863412645, The Institution of Engineering and Technology.

[5] J. Eyer and G. Corey, Energy Storage for the Electricity Grid: Benefits and Market Potential Assessment Guide Sandia, NM, Sandia report SAND 2010-0815, 2010.

[6] Makarov Y V, Du P, Kintner-Meyer M C W, et al. Sizing energy storage to accommodate high penetration of variable energy resources[J]. Sustainable Energy, IEEE Transactions on, 2012, 3(1): 34-40.

[7] Fanliang B, Control method of hybrid ESS combination of super capacity and battery in PV system[D]. Taiyuan University of Technology, 2011

[8] Zhenwei W, Xiaoping J, Huimeng M, et al. For wavelet hybrid energy storage to stabilize the PV fluctuation packet fuzzy control[J]. Journal of Chinese Electrical Engineering Science, 2014, 34(1): 317-324.

[9] Chen H, Cong T N, Yang W, et al. Progress in electrical energy storage system: A critical review[J]. Progress in Natural Science, 2009, 19(3): 291-312.

[10] Electrical energy storage: white paper. Technical report. Prepared by electrical energy storage project team. International Electrotechnical Commission (IEC), Published December 2011. <http://www.iec.ch/whitepaper/pdf/iecWP-energystorage-LR-en.pdf> [accessed 15.05.14].

[11] Brito AV, editor. Dynamic modelling. Molina MG. Chapter 4: Dynamic modelling and control design of advanced energy storage for power system applications. InTech; 2010. M.G.

[12] A. Price, S. Bartley, S. Male, G. Cooley, “A Novel Approach to Utility Scale Energy Storage”, Power Engineering Journal, Vol. 13, Issue 3, pp 122-129, June 1999

[13] John O. G. Tande, “Grid Integration of Wind Farms”, Wind Energy Vol. 6, No. 3, pp 281-295, September 2003

[14] “Variability of Wind Power and other Renewables: Management Options and Strategies”, International Energy Agency Publications, June 2005

[15] N. Hamsic, A. Schmelter, A. Mohd, E. Ortjohann, E. Schultze, A. Tuckey, J. Zimmermann, “Increasing Renewable Energy Penetration in Isolated Grids Using a Flywheel Energy Storage System”, Proceedings of Powereng 2007 - International Conference on Power Engineering, Energy and Electrical Drives, Setúbal, April 2007

[16] Faias S, Santos P, Sousa J, et al. An overview on short and long-term response energy storage devices for power systems applications[J]. system, 2008, 5: 6.

[17] N.S. Zhai, Y.Y. Yao, D.I. Zhang, D.G. Xu, “Design and Optimization for a Supercapacitor Application System”, International Conference on Power System Technology, pp. 1-4, October 2006

[18] A. Rufer, D. Hotellier, P. Barrade, “A Supercapacitor-Based Energy Storage Substation for Voltage Compensation in Weak Transportation Networks”, IEEE Transactions on Power Delivery, Vol. 19, N0. 2, pp 629-636, April 2004

[19] Toshiyuki Mito, “Development of UPS-SMES as a Protection From Momentary Voltage Drop”, IEEE Transactions on Applied Superconductivity, Vol. 14, N0. 2, pp 721-726, June 2004

[20] J. C. Smith, M. R. Milligan, E. A. DeMeo, and B. Parsons, “Utility wind integration and operating impact state of the art,” IEEE Trans. Power Syst., vol. 22, no. 3, pp. 900–908, Aug. 2007.

[21] Kelin Y, Ruiwen H, Haoming L, Control method of ESS in PV system to smooth the output power fluctuation, Electric Power Demand Side Management [J]. vol. 17, no. 2, pp. 17–21, 2015.

[22] Alvarado F L. Spectral analysis of energy-constrained reserves[C]//System Sciences, 2002. HICSS. Proceedings of the 35th Annual Hawaii International Conference on. IEEE, 2002: 749-756.

[23] Charles Van Loan, Computational Frameworks for the Fast Fourier Transform (SIAM, 1992).

[24] https://en.wikipedia.org/wiki/State_of_charge

[25] Carnegie R, Gotham D, Nderitu D, et al. Utility scale energy storage systems[J]. State Utility Forecasting Group. Purdue University, 2013, 1.

[26] Li B, Chen S, Liang S Y. A Suitable Method of Energy Storage Capacity Optimization Based on DFT for BIPV[C]//Applied Mechanics and Materials. 2014, 548: 901-909.

[27] Masters G M. Renewable and efficient electric power systems[M]. John Wiley & Sons, 2013.

[28] Shannon C E. Communication in the presence of noise[J]. Proceedings of the IRE, 1949, 37(1): 10-21.

[29] Yang R, Yang H, Ou W. Application of Special Optical Fiber Sensing Technology in New Generation of Smart Substation[J]. Advanced Materials Research, 2014.

[30] http://batteryplusforlife.com/research.html

[31] http://www.nrel.gov/electricity/transmission/pdfs/second_grid_sim_zagoras.pdf

[32] Davide Andrea (2010). Battery Management Systems for Large Lithium Ion Battery Packs. Artech House. p. 189. ISBN 978-1-60807-105-0. Retrieved 19 June 2013.

[33] Xia Y, Zhou Y, Yoshio M. Capacity Fading on Cycling of 4 V Li/LiMn2 O 4 Cells[J]. Journal of The Electrochemical Society, 1997, 144(8): 2593-2600.

[34] Amatucci G G, Tarascon J M, Klein L C. Cobalt dissolution in LiCoO 2-based non-aqueous rechargeable batteries[J]. Solid State Ionics, 1996, 83(1): 167-173.